Gold nanoparticles: From nanomedicine to nanosensing

Po C Chen
Sandra C Mwakwari
Adegboyega K Oyelere

School of Chemistry and Biochemistry, Parker H Petit Institute for Bioengineering and Bioscience, Atlanta, GA, USA

Abstract: Because of their photo-optical distinctiveness and biocompatibility, gold nanoparticles (AuNPs) have proven to be powerful tools in various nanomedicinal and nanomedical applications. In this review article, we discuss recent advances in the application of AuNPs in diagnostic imaging, biosensing and binary cancer therapeutic techniques. We also provide an eclectic collection of AuNPs delivery strategies, including assorted classes of delivery vehicles, which are showing great promise in specific targeting of AuNPs to diseased tissues. However, successful clinical implementations of the promised applications of AuNPs are still hampered by many barriers. In particular, more still needs to be done regarding our understanding of the pharmacokinetics and toxicological profiles of AuNPs and AuNPs-conjugates.

Keywords: gold nanoparticles (AuNPs), targeted delivery, receptor-mediated endocytosis (RME), near infrared (NIR), surface plasmon resonance (SPR), surface-enhanced Raman scattering (SERS), bioimaging, biosensing, photothermal therapy

Introduction

Some of the challenges facing conventional therapies are poor bioavailability and intrinsic toxicity. These have seriously compromised the therapeutic efficacy of many otherwise beneficial drugs. Nanoscopic systems that alter the pharmacological and therapeutic properties of molecules are being designed to overcome some of these limitations. Research efforts in this area have resulted in innovative nanodevices and nanostructures for use in applications such as diagnostics, biosensing, therapeutics, and drug delivery and targeting (Sahoo and Labhasetwar 2003; Freitas 2005; Kawasaki and Player 2005; Koo et al 2005; Cheng et al 2006; Peters 2006; Baron et al 2007; Villalonga et al 2007; Heath and Davis 2008).

Drug delivery with nanotechnological products takes advantage of pathophysiological conditions and anatomical changes within diseased tissues, compared with normal tissues, to achieve site-specific and targeted delivery (Sahoo et al 2007; Prato et al 2008). Nanosystems are often accumulated at higher concentrations than normal drugs, thereby enhancing bioavailability at the targeted site. The enhanced drug targeting to the diseased tissues usually leads to reduced systemic toxicity. Moreover, incorporation of drug molecules in nanosized systems could improve drug solubility; offer a regulated drug release with enhanced retention at the target sites. These unique properties of nanosystems have been exploited to deliver drugs to harder-to-target sites such as the brain which offers a challenge due to the presence of the blood–brain barrier (Maeda et al 2000; Mu and Feng 2003; Sahoo and Labhasetwar 2003; Torchilin et al 2003; Rawat et al 2006; Sahoo et al 2007). Several varieties of engineered nanoparticles (Table 1) have been widely used for drug delivery, imaging, biomedical diagnostics, and therapeutic applications (Sahoo and Labhasetwar 2003; Chen et al 2005; Loo et al 2005; Yeh et al 2005; Huang et al 2006; Lee and Wang 2006; Rawat et al 2006; Dong and Roman 2007; Lu et al 2007; Maysinger 2007; Oyelere et al 2007; Sahoo et al 2007;

Correspondence: Adegboyega K Oyelere
School of Chemistry and Biochemistry, Parker H Petit Institute for Bioengineering and Bioscience, Atlanta, GA 30332-0400, USA
Tel +1 404 894 4047
Fax +1 404 894 2291
Email aoyelere@gatech.edu

Table 1 Examples of nanoscale scaffolds for medical applications

Nanoparticle	Example	Medical application	References
Metal nanoparticles	Quantum dots Gold nanoparticles Gold nanorods Gold nanoshells Gold nanocages	Diagnostics Biosensor Molecular imaging Drug delivery	Chen et al 2005; Loo et al 2005; Yeh et al 2005; Huang et al 2006; Baron et al 2007; Maysinger 2007; Oyelere et al 2007; Skrabalak et al 2007; Villalonga et al 2007; Cho et al 2008
Nanotubes and nanowires	Carbon-nanotubes	Biomolecular sensing Delivery of vaccines or proteins	Baron et al 2007; Maysinger 2007; Cho et al 2008
Dendrimers	Poly(amido) amine PAMAMs	Drug carriers Imaging agents Gene delivery	Rawat et al 2006; Maysinger 2007; Villalonga et al 2007; Cho et al 2008
Liposomes	(PEG)ylated immunoliposomes	Drug delivery Gene encoding	Rawat et al 2006; Villalonga et al 2007; Cho et al 2008
Polymeric micelles	[PEG-PAsp (DOX)] Doxorubicin conjugated to poly(ethylene glycol)-poly (α, β-aspartic acid)	Drug delivery of water-insoluble drugs	Sahoo and Labhasetwar 2003; Cho et al 2008
Ceramic nanoparticles	Silica-based nanoparticle entrapping photosensitizing anticancer drug, 2-devinyl-2-(1-hexyloxyethyl) pyropheophorbide	Drug delivery	Sahoo and Labhasetwar 2003
Polymeric nanoparticles	PLGA (Poly(D, L-lactic-coglycolic acid)) PLA-PGA (Poly-L-glutamic acid)	Drug delivery Protein delivery Gene expression vector	Rawat et al 2006; Sahoo et al 2007; Villalonga et al 2007; Cho et al 2008
Polysaccharide nanoparticles	Cellulose nanocrystals	Targeted delivery Bioimaging	Dong and Roman 2007; Villalonga et al 2007
Magnetic nanoparticles	Superparamagnetic iron oxide	Magnetic Resonance Imaging contrast agents	Baron et al 2007; Lu et al 2007
Bionanoparticles (BNPs) – Protein-based nanosystems	Ferritin Viruses and virus-like particles Heat shock protein cages	Gene delivery Bioimaging Drug delivery Vaccine development	Lee and Wang 2006

Skrabalak et al 2007; Cho et al 2008). Due to their small size (10 nm to 100 nm) (Sahoo et al 2007), several of these nanoparticles can penetrate smaller capillaries and are up taken by the cells. Many are also known to be biocompatible, undetected by the immune system, and biodegradable. Additionally, many could possess unique optical and electrical properties (Maysinger 2007), key examples include quantum dots (Q-dots) and gold nanoparticles (AuNPs), making it possible to track their intracellular trafficking and localization (Maysinger 2007; Oyelere et al 2007).

For drug delivery applications, the drug of interest is either encapsulated, entrapped, adsorbed, attached, or dissolved into the nanoparticle matrix for release at the specific site (Sahoo and Labhasetwar 2003). An emerging trend in this field is the development of multifunctional nanoparticles. For example, polymeric micelles, which act as cancer-targets, drug delivery agents and possess magnetic resonance imaging (MRI) contrast characteristics, have been reported (Nasongkla et al 2006). Majoros and colleagues (2006) have synthesized and characterized a multifunctional dendrimer conjugated with fluorescein isothiocyanate (for imaging), folic acid (for targeting cancer cells overexpressing folate receptors), and paclitaxel (chemotherapeutic drug).

Recent advances in the use of nanoparticles in medicine include delivery of antigens for vaccination (Pulliam et al 2007), gene delivery for treatment or prevention of genetic disorders (Ragusa et al 2007), and other therapeutics such as in cardiac therapy (Lanza et al 2006; Brito and Amiji 2007), dental care (Bakó et al 2007), and orthopedic applications (Streicher et al 2007). This has been the subject of many influential reviews (Lanza et al 2006; Han et al 2007; Morrow et al 2007; Sahoo et al 2007; Jain 2008). The focal point of

the current review is to discuss the current use of AuNPs in medicine specifically, including targeted drug delivery, biosensing and bioimaging, and photothermal therapy.

Historic perspective on the use of AuNPs in medicine

Chrysotherapy, the use of gold in medicine, has been practiced since antiquity. Ancient cultures such as those in Egypt, India, and China used gold to treat diseases such as smallpox, skin ulcers, syphilis, and measles (Huaizhi and Yuantao 2001; Richards et al 2002; Gielen and Tiekink 2005; Kumar 2007). Presently, gold is in use in medical devices including pacemakers and gold plated stents (Edelman et al 2001; Svedman et al 2005), for the management of heart disease; middle ear gold implants (Thelen et al 2006), and gold alloys in dental restoration (Demann et al 2005; Svedman et al 2006). In the past few decades, several organogold complexes have emerged with promising antitumor, antimicrobial, antimalarial, and anti-HIV activities (Shaw 1999; Gielen and Tiekink 2005; Sun et al 2007). In fact, organogold compounds are now widely used for the treatment of rheumatoid arthritis (Shaw 1999; Moolhuizen et al 2004; Sun et al 2007). Organogold compounds relieve arthritis symptoms such as joint pain, stiffness, swelling, bone damage, and also reduce the chance of joint deformity and disability. However, many of these compounds have shown reversible dose-dependent toxicities. In particular, at high doses, arthritis patients undergoing chrysotherapy often experience two common side effects: proteinuria and skin reactions (Moolhuizen et al 2004).

Synthesis of AuNPs and its alloys

Several methods have been described in the literature for the synthesis of AuNPs of various sizes and shapes. The most popular synthetic method is by chemical reduction of gold salts such as hydrogen tetrachloroaurate ($HAuCl_4$) using citrate as the reducing agent (Frens 1973). This method produces monodisperse spherical AuNPs in the 10–20 nm diameter range. However, production of larger AuNPs (40–120 nm) by this method proceeds in low yields, often resulting in polydisperse particles. Brown and Natan (1998) have reported the synthesis of monodisperse AuNPs with diameters between 30 and 100 nm using a seeding approach. The method is based on the use of the surface of AuNPs as a catalyst for the reduction of Au^{3+} by hydroxylamine. Subsequently, Murphy and colleagues employed this seed-mediated growth approach to control the shape and size of the nanoparticles (Jana et al 2001a, 2001b). Borohydride-reduced AuNPs seeds (3–4 nm diameter) were mixed with gold salt growth solution, rod-shaped micellar template (cetyltrimethylammonium bromide; CTAB), reducing agent (ascorbic acid), and small amount of silver ions for shape induction to produce spheroid or rod-like gold nanoparticles (Jana et al 2001a, 2001b). They have also improved this methodology to produce monodisperse, multiple-shaped AuNPs in higher yields than previously reported (Busbee et al 2003; Sau and Murphy 2004).

Other methods for the synthesis of AuNPs include physical reduction (Sun et al 2003) (hollow Au nanostructures in large-scale), photochemical reduction (Kundu et al 2007) (cubic AuNPs), biological reduction (Mitra and Das 2008) (molecular hydrogels of peptide amphiphiles for producing various shapes of AuNPs), and solvent evaporation techniques (Pyrpassopoulos et al 2007) (2D Au super lattices). Recently, a simple and potentially cost effective microwave irradiation approach for the synthesis of shape-controlled AuNPs was reported (Kundu et al 2008). In this approach, irradiation of Au salt, reduced in CTAB micellar media, in the presence of alkaline 2,7-dihydroxy naphthalene (2,7-DHN), generate exclusively spherical, polygonal, rods, and triangular AuNPs within 90 seconds.

Bimetallic AuNPs, such as Au–Ag, have also attracted attention due to their interesting catalytic, structural and electronic properties, and the sensitivity of their surface plasmon resonance (SPR) properties (Huang et al 2004; Lee and El-Sayed 2006). Accordingly, the development of simple and robust methods for the synthesis of bimetallic nanoparticles is currently of great interest. Spherical Au/Ag alloy nanoparticles whose SPR band could easily be tuned by varying the molar fractions of gold could be obtained by reduction of Au and Ag salt with sodium citrate in refluxing aqueous solution (Sun and Xia 2003). A seed-mediated approach (Lu et al 2002; Sun and Xia 2003) to synthesize Au-Ag core-shell nanorods from silver ions, using gold nanorods as seeds, has also been reported. Other methods for the synthesis of bimetallic AuNPs include sputter deposition technique in ionic liquids (Okazaki et al 2008), photochemical synthesis (Pal and Esumi 2007), and deposition of Au/Ag on silica (Pal and De 2007). Relatively recently, a reverse microemulsion method to prepare silica-coated Au–Ag nanoparticles has been developed (Han et al 2008).

Over the years, the ease of fabrication and the unique chemical and optical properties have sustained interests in the use of AuNPs in various molecular imaging and delivery applications. More significantly, the unique biodistribution of AuNPs within tumors have led to the discovery of gold-based

nanosystems as delivery vehicles for chemotherapeutic agents (Paciotti et al 2006).

Bioimaging

Researchers have used various exogeneous agents to visualize key subcellular compartments. Cell imaging is achieved through the generation of colorimetric contrast between different cells/subcellular organelles by these imaging agents. Conventional exogeneous imaging agents include lanthanide chelates and organic fluorophores (Sharma et al 2006). However, organic fluorophores are prone to photobleaching, low quantum yields, and broad emission window (Bruchez et al 1998; Chan et al 2002). Lanthanide chelates, on the other hand, are prone to nonselective localization in extravascular space (Sharma et al 2006). The shortcomings of the conventional imaging agents have limited their applications as biomedical diagnostic tools and have stimulated interest in typical nanomaterials, such as magnetic nanoparticles (Kim et al 2003; Martina et al 2005; Lee et al 2006b), Q-dots (Akerman et al 2002; Kim et al 2004; Gao et al 2005), and AuNPs (Boyer et al 2002; Cognet et al 2003; Loo et al 2005; Huang et al 2006; Ipe et al 2006; Lewis et al 2006; Qian et al 2008) as alternative contrasting agents. These nanomaterials are optimal diagnostic tools since they eliminate most of the vulnerabilities of the conventional imaging agents. However, the intrinsic cytotoxicity of most nanomaterials has diminished their utility in many *in vitro* and *in vivo* application (El-Sayed et al 2005b; Thurn et al 2007; Lewinski et al 2008). AuNPs are unique exceptions because they are more tolerable and compatible with cellular environment (Tkachenko et al 2003; Connor et al 2005; Shukla et al 2005; Pan et al 2007). In addition, the colorimetric contrast observed within the AuNPs treated cells could be controlled by size (Turkevich et al 1951; Kreibig and Genzel 1985; Khlebtsov et al 2005), shape (Sarkar and Halas 1997; Jin et al 2001; Murphy and Jana 2002), or even surface modification (Marinakos et al 1999; Caruso and Antonietti 2001) of the AuNPs due to a phenomenon called surface plasmon resonance (SPR) (Sharma et al 2006). When excited, the SPR of AuNPs could scatter and/or absorb light in the visible or the near-infrared (NIR) spectrum (Jain et al 2006), an extremely useful property for *in vivo* optical imaging techniques such as photoacoustic (Agarwal et al 2007), and two-photon luminescence imaging (Durr et al 2007). These two optical diagnostic techniques specifically generate cellular contrast by tuning the SPR of the AuNPs to the NIR spectrum. Other noninvasive diagnostic tools such as MRI (Debouttiere et al 2006) and X-ray computed tomography (X-ray CT) (Kim et al 2007) have utilized AuNPs as contrasting agent due to the ease of surface modification and higher X-ray absorption coefficient, respectively.

Magnetic resonance imaging

Magnetic resonance imaging is a noninvasive diagnostic tool that applies magnetic fields to the heterogeneous composition of water in organisms (Weissleder and Mahmood 2001; Caravan et al 2003; Langereis et al 2004). Different water proton relaxivity rates translate into contrasting images of different cells (Debouttiere et al 2006). The MRI images can be enhanced by reducing the longitudinal and transverse relaxation time of the water proton (Caravan et al 1999; Merbach and Toth 2001). The enhancement is often observed by the use of contrasting agents such as gadolinium chelates (Caravan et al 1999) or superparamagnetic iron oxide (Aime et al 1998). The most widely used contrasting agent for MRI is gadolinium-diethyltriaminepentaacetic acid (Gd-DTPA) (Sharma et al 2006). In this reagent, Gd^{III} is the contrasting agent, while DTPA is the chelating ligand that forms a complex with Gd^{III} to minimize the leaching of the cytotoxic, ionic Gd^{III} into the cellular milieu (Figure 1). Despite the contrast enhancement, the imaging application of Gd-DTPA is still hampered by their rapid renal clearance (Debouttiere et al 2006). For optimal contrast enhancement, AuNPs have been utilized as a delivery vehicle to convey multiple Gd-DTPA complexes into selective cellular targets. Dithiolated DTPA (DTDTPA) has been utilized in place of DTPA to chelate to ionic Gd^{III} and permit conjugation onto 2 to 2.5 nm AuNPs surface (Figure 2). In the MRI study performed by Roux and colleagues, Gd-DTDTPA/AuNPs conjugates retain the intrinsic contrasting property of Gd-DTPA under MRI and provide the desired contrast enhancement compared to single Gd-DTPA (Debouttiere et al 2006). However, the *in vivo* application and cytotoxicity of the Gd-DTDTPA/AuNPs conjugates have not been fully investigated (Debouttiere et al 2006).

X-ray computed tomography

X-ray computed tomography is another noninvasive diagnostic method that generates three-dimensional images of different cells based on a series of two-dimensional X-ray images compiled around a single rotating axis (NCI 2003). Contrasting agents are often utilized to enhance the contrast between cells because of their affinity to absorb X-rays. One of the widely used contrasting agents in X-ray CT is called Ultravist (iopromide), an iodinated small molecule dye

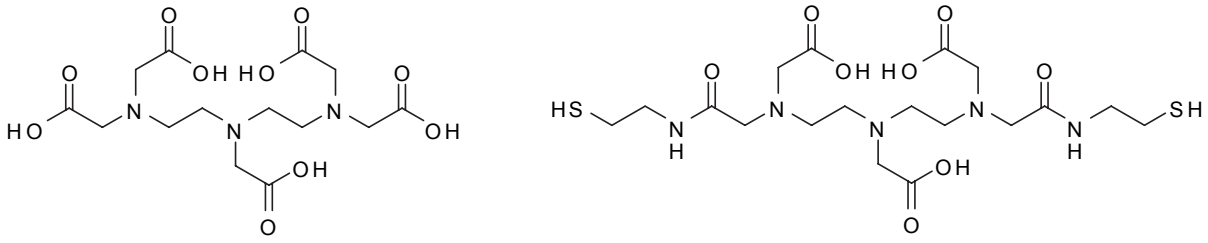

Diethylenetriaminepenta acetic acid
(DTPA)

Dithiolated diethylenetriaminepenta acetic acid
(DTDTPA)

Figure 1 Chemical structures of DTPA (left), and DTDTPA (right).

(Figure 3) (Kim et al 2003). There are several shortcomings of Ultravist that includes renal toxicity (Hizoh and Haller 2002; Haller and Hizoh 2004), vascular permeation, and limited imaging interval due to rapid renal execretion (Kim et al 2007). The limitations observed in current CT contrasting agents were recently overcome by the use of AuNPs. AuNPs present several advantages over the current contrasting agents, such as higher X-ray absorption coefficients (Hainfeld et al 2006), versatility in surface modification, and regulated control in the size and shape of the AuNPs. Recently, Kim and colleagues (2007) performed CT studies on AuNPs coated with poly-ethylene gycol (PEG) (Allen et al 1991; Papahadjopoulos et al 1991; Herrwerth et al 2003; Zheng et al 2003; Ballou et al 2004; Kohler et al 2004; Lee et al 2006a) as antibiofouling agents, to test their *in vivo* application as CT contrast agents for angiography and hepatoma detection. X-ray absorption coefficient measurements *in vitro* revealed that the attenuation of PEG-coated AuNPs is 5.7 times higher than Ultravist at equal concentration. The PEG-coated AuNPs have a longer blood circulation time, approximately 4 hours without apparent loss of contrast in a mice model, compared with only about 10 minutes for Ultravist. Also, a two-fold contrast enhancement was seen between the hepatoma and its surrounding healthy liver cells for up to 24 hours. These results showed the feasibility of AuNPs as a CT contrast agent *in vivo*. Although no considerable

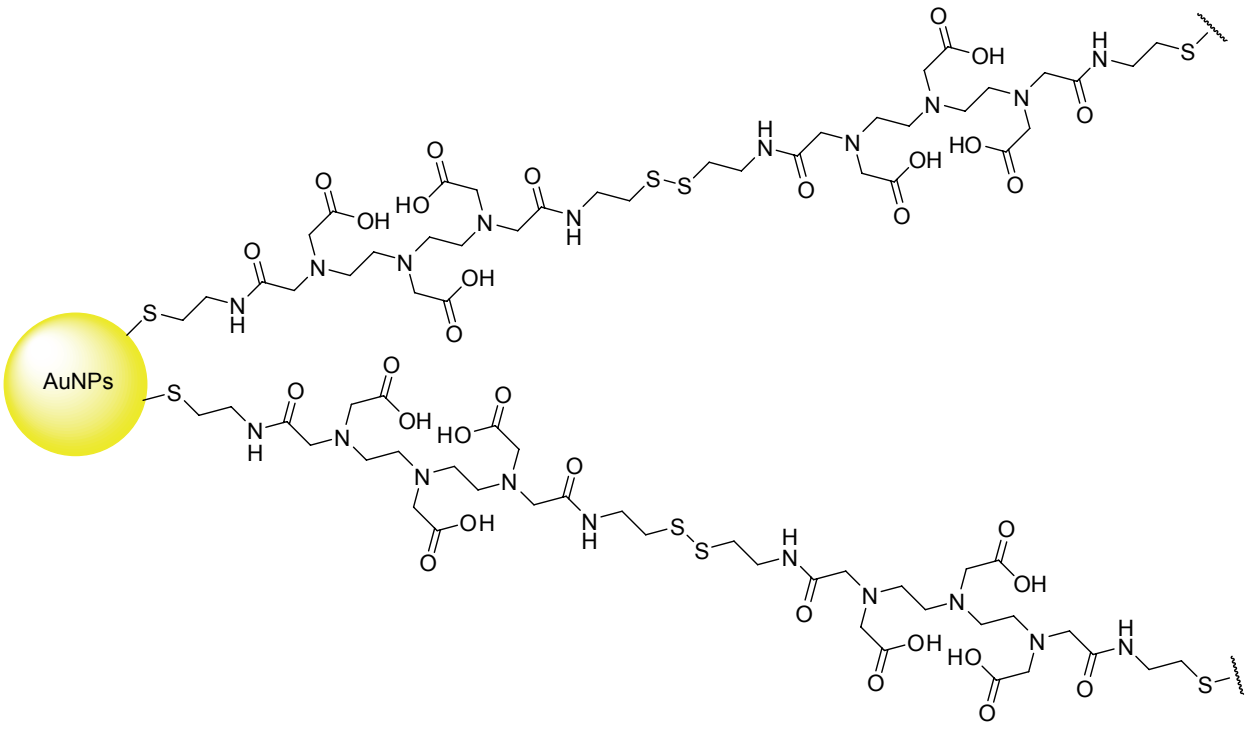

Figure 2 Schematic illustration of DTDTPA–AuNPs.

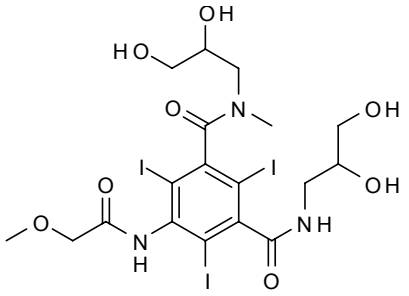

Ultravist (iopromide)

Figure 3 Chemical structure of Ultravist (iopromide), a contrast agent used in X-ray computed tomography.

toxicity was detected in liver cells (HepG2) upon exposure to the PEG-coated AuNPs for 24 hours, further studies need to be undertaken for PEG-coated AuNPs to be considered a clinically useful contrast agent.

Optical imaging

In photoacoustics (Agarwal et al 2007) and two-photon luminescence (Durr et al 2007), AuNPs are utilized as contrasting agent that permits light scattering and/or absorption at the NIR spectrum (between 700–1000 nm) (Agarwal et al 2007). This imaging window is known as the "tissue transparency window". Light penetration at this imaging window is at maximum with minimum loss to hemoglobin and water absorption, thereby permitting deep imaging of the cells (Mahmood and Weissleder 2003). Agarwal and colleagues (2007) used 15-nm AuNPs in a photoacoustic experiment to enhance cell contrast upon irradiation by a short pulse laser. The acoustic emissions created by the AuNPs are collected by ultrasonic array to recreate the initial heat distribution that images the target cell. AuNPs efficiently emit two-photon luminescence because they can sustain SPR with little or no damping after the photon excitation (Sonnichsen et al 2002). The two-photon cross sections of AuNPs have been exploited in two-photon luminescence experiments to image target cells (Wang et al 2005). With appropriate delivery platforms on the AuNPs, photoacoustics (Agarwal et al 2007) and two-photo luminescence imaging (Durr et al 2007) have been used to selectively image LnCAP prostate cancer and A431 skin cancer cells, respectively. Most of the delivery platforms in optical diagnostic application are protein- and peptide-based, these will be discussed later in this review.

Biosensing

Biosensors employ biological molecules such as antibodies, enzymes, carbohydrates, and nucleic acids to identify or follow the course of any biological phenomena of interest (Otsuka et al 2001; McFadden 2002). Interactions, such as hydrogen bonding and charge–charge transfers between the ligand and receptor molecules, coupled with read-out techniques such as colorimetry, fluorescence, biomagnetic signals, etc, are used for sensing specific biochemical events (McFadden 2002). Biosensors are finding use in various applications: food processing, to monitor food-borne pathogens in the food supply; environmental monitoring, to detect pollutants and pesticides in the environment; biowarfare defense, to detect bacteria, viruses and biological toxins; and clinical diagnostics, to measure blood glucose levels (McFadden 2002; Li and Rothberg 2004).

AuNPs exhibit special optical and electronic properties such as enhanced SPR, surface-enhanced emission, and surface-enhanced Raman scattering (SERS) (Frederix et al 2003; Huang et al 2007a). These properties have been used in sensing and/or monitoring numerous molecular events including protein–protein interaction, protein aggregation, and protein folding (De et al 2007; Ghoshmoulick et al 2007; Villalonga et al 2007). For example, the SPR signals of AuNPs have been used not only to selectively detect DNAs but also to differentiate between perfect and mismatched DNA duplex. Mirkin and colleagues reported that mercaptoalkyloligonucleotide-modified AuNPs probes generate cross-linked polymeric aggregates that signaled hybridization with complementary oligonucleotide target via color change (Elghanian et al 1997). The color of the nanoparticle aggregates appeared to vary as the interparticle distance changes; a phenomenon attributed to the SPR of Au (Elghanian et al 1997). Moreover, the colorimetric transition temperatures of the nanoparticle aggregates were used to differentiate a perfect match target from a mismatch base target. However, this approach is limited in that it is inherently a one-color system that is based on a gray scale. A system that overcomes this handicap, by performing multiplexed detection of oligonucleotide targets, has been reported (Cao et al 2002). This system consists of 13-nm AuNPs probes functionalized with oligonucleotides and Raman-dye labels as Raman spectroscopic fingerprint. It distinguishes between oligonucleotide sequences using Ag surface-enhancement of SERS as readout. Several dissimilar DNA targets and two RNA targets were distinguished (Cao et al 2002).

A new aggregation phenomenon of DNA-functionalized AuNPs, induced by noncross-linking target DNA hybridization, has been recently reported. This phenomenon allows simple and rapid colorimetric sensing of DNA hybridization that is sufficiently sensitive to detect terminal single-base-pair mismatches

(Sato et al 2003, 2005; Li and Rothberg 2004). Based on its simplicity and easy read-out (Sato et al 2003), this technique has opened up a new possibility for reliable genetic diagnosis. Another colorimetric hybridization assay that uses unmodified/unfunctionalized AuNPs for sequence-specific detection of DNA has appeared in the literature (Li and Rothberg 2004). Based on the differences in electrostatic properties between single stranded DNA (ssDNA) and double stranded DNA (dsDNA), ssDNA selectively adsorbs on and stabilizes the AuNPs against aggregation in high salt buffers relative to dsDNA. This assay has an added advantage of being completely independent of the detection step while adaptable to sensing single-base-pair mismatches between probe and target.

AuNPs colorimetric response to changes in environment has been extended to detection of protein–ligand interactions (Tsai et al 2005). For example, concanavalin (ConA)–mannose interaction has been investigated using mannose modified–AuNPs (Man–AuNPs). It was demonstrated that the interaction between ConA and Man–AuNPs resulted in aggregation (blue colored aggregates) suggesting specific binding of Man–AuNPs to ConA. To further probe the specificity of this interaction, a variety of proteins were added to the Man–AuNPs/ConA aggregate, and it was shown, via colorimetric response (blue to burgundy = loss of aggregation), that a subset of these proteins effectively compete with ConA for Man–AuNPs binding. The system is sensitive within a nanomolar range and potentially could be applied to investigate a broad range of protein–ligand interactions.

AuNPs/enzymes-based biosensors that measure cellular glucose levels have also been developed for potential use in diabetes management (Stonehuerner et al 1992; Aubin et al 2005; Ha et al 2005; Simonian et al 2005; Hill and Shear 2006; Jena and Raj 2006; Zhao et al 2008). These sensors use glucose oxidase immobilized on AuNPs to detect glucose concentrations (Pandey et al 2007). AuNPs immobilization of glucose oxidase resulted in glucose sensors with enhanced sensitivity and stability. Using AuNPs to which a yeast iso-1-cytochrome c (Cytc) is covalently attached, Zare and collegues have demonstrated that AuNPs could be used as a colorimetric sensor to follow the folding or unfolding of an appended protein molecule (Chah et al 2005). Upon exposure to buffers of different pH, the appended Cytc unfolds at low pH, thus inducing AuNPs aggregation while refolding at high pH, results in the loss of aggregation. These conformational changes caused measurable shifts in the AuNPs' color and could be detected by UV–VIS absorption spectroscopy (Chah et al 2005). In a similar manner, the pH dependent shifts in the AuNPs plasmon resonance have recently been used to track protein structural changes induced by glycation (Ghoshmoulick et al 2007), a modification that is of importance in the clinicopathology of diabetes (Hudson et al 2002). Glycation progress was found to correlate with a significant shift in the size distribution of AuNPs as well as their plasmon resonance peak and intensity.

Photothermal therapy

Photothermal therapy is a less invasive experimental technique that holds great promise for the treatment of cancer and related disease conditions (Huang et al 2006). It combines two key components: (i) light source, specifically lasers with a spectral range of 650–900 nm (Huang et al 2006) for deep tissue penetration, and (ii) optical absorbing AuNPs which transform the optical irradiation into heat on a picosecond time scale, thereby inducing photothermal ablation (Chen et al 2007a; Haba et al 2007). Recent developments have shown that the spectral signature of AuNPs could be tailored or tuned by altering their shape or size. El-Sayed and colleagues have demonstrated that gold nanorods have a longitudinal absorption band in the NIR on account of their SPR oscillations and are effective as photothermal agents (Huang et al 2006). Other gold nanostructures such as gold nanoshells (Loo et al 2005), gold nanocages (Chen et al 2007a), and gold nanospheres (Huang et al 2008) (Figure 4) have also demonstrated effective photothermal destruction of cancer cells and tissue. However, efficient *in vivo* targeting of AuNPs to heterogeneous population of cancer cells and tissue still requires better selectivity and noncytotoxicity to surrounding normal cells.

Selectivity

Although nanoparticle-based therapeutics exploits the enhanced permeability and retention (EPR) effect for delivery into tumors, not all tumors are amenable to this effect, especially in regard to the delivery of the nanoparticles of relatively large size (Ishida et al 1999). In addition, selective photothermolysis is not obtained for small tumors or single metastatic cells because heat diffusion from hot particles increases the damaged tissue area with longer exposure times (Zharov et al 2005). Hence, other methods of selective nanoparticle delivery need to be developed in order to achieve effective photothermal therapy. Recent studies have shown that AuNPs conjugated to antibodies (Huang et al 2006) and viral vectors (Everts et al 2006) could be used for selective and efficient photothermal therapy. Huang and colleagues (2006) have demonstrated

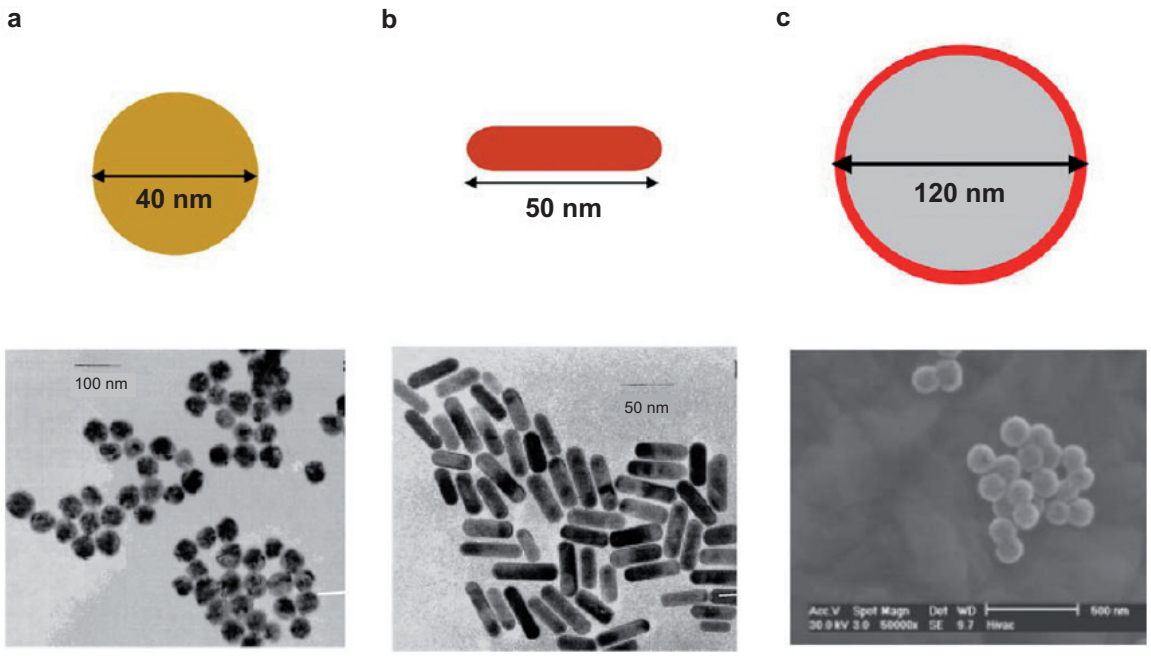

Figure 4 TEM images of plasmonic gold nanostructures commonly used for PPTT. **a**) nanospheres, **b**) nanorods, **c**) nanoshells.

that gold-nanorods conjugated to anti-epidermal growth factor receptor (anti-EGFR) antibodies selectively target cell lines that overexpress EGFR. Subsequent continuous laser exposure of nanoparticle-treated cells resulted in photothermal destruction of the EGFR positive cells at half the energy required to kill EGFR negative cells. Similarly, treatment of breast cancer cell line overexpressing HER2 with HER2-targeted gold nanoshells (Hirsch et al 2003; Lowery et al 2006; Bernardi et al 2008) and nanocages (Chen et al 2007a) followed by exposure to laser light in the NIR has been shown to selectively induce cell death to the HER2 positive cell *in vitro*.

The potential of photothermal therapy in disease intervention has recently been extended to include parasite infections. Using gold nanorods conjugated with antibody selective for *Toxoplasma gondii*, Pissuwan and colleagues (2007) reported that plasmonic heating with a 650-nm laser at power density of 51 W/cm^2 resulted in more than 80% destruction of *T. gondii* tachyzoites. This is one of the early examples of photothermal intervention in parasitic diseases; more studies need to be done to ascertain its general utility.

Toxicity

Organogold antiarthritis compounds, such as auranofin and Tauredon (Figure 5), have presented some dose-dependent adverse side effects. Nevertheless, AuNPs are generally considered to be benign. However, the size similarity of AuNPs to biological matters could provide "camouflage" to cellular barriers, leading to undesired cellular entry which might be detrimental to normal cellular function (Connor et al 2005). The prospect that the inadvertent AuNPs' cellular entry could result in toxic side effects have stimulated intense efforts aimed at providing better insight into their toxicity profile. Pan and colleagues (2007) recently conducted a systematic investigation of the size-dependent cytotoxicity of water soluble, triphenylphosphine-stabilized AuNPs against four cell lines: Hela cervix carcinoma epithelial cells, Sk–Mel–28 melanoma cells, L929 mouse fibroblast, and J774A1 mouse monocytic/macrophage cells. They found that AuNPs 1 to 2 nm in size displayed cell-type dependent cyotoxicity with high micromolar IC_{50}s. In contrast, AuNPs 15 nm in size were nontoxic

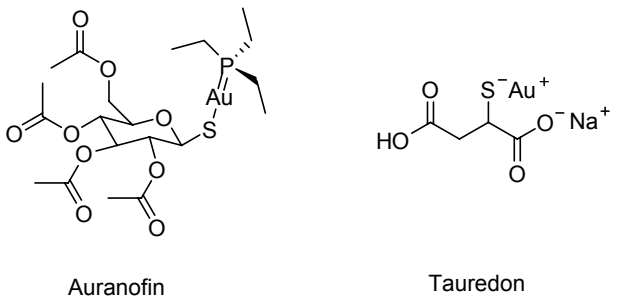

Figure 5 Examples of chrysotherapeutics utilized in rheumatoid arthritis treatment. Chemical structures of auranofin (left) and Tauredon (right).

to cells at concentrations 60-fold higher than the IC_{50} of the smaller AuNPs. These results seemed to confirm size-dependent toxicity of AuNPs (Paciotti et al 2004; El-Sayed et al 2005a, 2005b; Debouttiere et al 2006; Huang et al 2006, 2007b; Visaria et al 2006; Kim et al 2007; Nicholas et al 2007), an inference that has hitherto been somewhat ambivalent.

Earlier investigation by Rotello and colleagues have shown that cationic side chains (CTAB) tend to impart moderate toxicity to AuNPs whereas anionic side chains (carboxylate-derived) are generally nontoxic (Figure 6) (Goodman et al 2004). Further analyses revealed that the toxicity observed with the cationic AuNPs is due to cell lysis rather than receptor-mediated endocytosis (RME). A later study by Connor and colleagues (2005) revealed that the CTAB-bound AuNPs by themselves do not present measurable toxicity to K-562 leukemia cell line. Instead, toxicity was due to the presence of unbound CTABs. This result suggested that the toxicity observed in Rotello's experiment could be the consequence of the unbound CTAB derivative.

Overall, current literature evidence support the assertion that AuNPs and their conjugates are relatively less toxic to cells (Tkachenko et al 2003; Connor et al 2005; Shukla et al 2005; Pan et al 2007; Lewinski et al 2008). Nevertheless, identification of proper delivery platforms will further enhance the prospects of AuNPs as tools for noninvasive disease diagnosis and treatment.

Delivery

Efficient delivery of AuNPs into a living system requires overcoming natural biological barriers such as the cell membrane and the reticuloendothelial system (RES). For specific tumor targeting, AuNPs face additional challenges from receptor specificity and intratumor barriers. Potential approach for optimizing AuNPs delivery is particle size reduction ("true nanometer scale") or acquisition of surface modification. For example, large AuNPs are quickly opsonized by blood and eliminated by the RES in mammalian cells (Woodle et al 1994; Raynal et al 2004; Roger and Basu 2005; Paciotti et al 2006). To bypass RES, antibiofouling agents such as

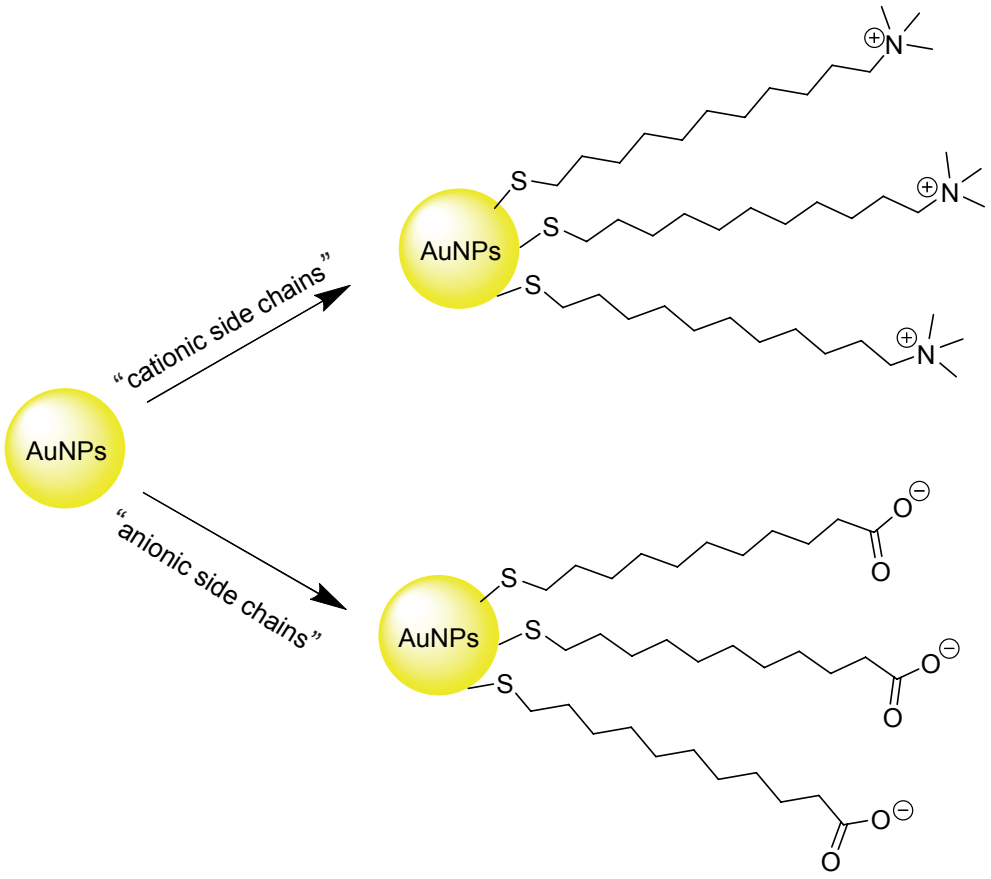

Figure 6 Cationic (CTAB-derived, top right) and anionic (carboxylate-derived, bottom right) side chain surface modification of AuNPs.

thiol-derivatized poly-ethylene glycol (PEG-SH) have been grafted onto AuNPs surface as secondary coating. It has been observed that this secondary coating could delay RES clearance to liver from 0.5 hours to 72 hours in a mice model, an approximately 150-fold improvement compared with the unmodified CTAB-capped AuNPs (Niidome et al 2006). Several investigators have grafted different delivery platforms onto AuNPs surface to attempt cellular selectivity, internalization, and localization within heterogeneous population of cancer cells in solid tumors. These delivery platforms generally consist of macromolecules such as proteins and peptides or small molecules such as folic acid and paclitaxel. Several of these platforms have shown very promising results in delivering AuNPs into solid tumors (El-Sayed et al 2005a, 2005b; de la Furente et al 2006; Huang et al 2006; Paciotti et al 2006; Visaria et al 2006).

Protein delivery platforms

Proteins such as tumor necrosis factor-α (TNFα) and anti-EGFR antibodies have been successfully grafted onto AuNPs surface and utilized in conjunction with hyperthermia to selectively kill cancer cells. Another protein that shows selective cellular intake into cancer cells when conjugated to AuNPs is transferrin. However, its therapeutic application is yet to be fully investigated (Yang et al 2005). In several of these protein–AuNPs conjugates, the protein component selectively penetrates cancer cells through RME (Paciotti et al 2006; Visaria et al 2006). TNFα provides an illustrative example in this regard.

TNFα is a potent cytokine that induces systemic inflammation. Additionally, TNFα is known to be overexpressed in solid tumors (Paciotti et al 2004) and mediates hemorrhagic necrosis in solid tumors (North and Havell 1988; Kircheis et al 2002; Paciotti et al 2006; Visaria et al 2006). The later property suggests TNFα may find use in cancer therapy. However, TNFα has low therapeutic index due to nonselective acute toxicity that results from cell exposure (Brouckaert et al 1986; Hieber and Heim 1994). Recent observations on selective uptake of AuNPs by tumors have enabled a re-evaluation of the potential application of TNFα in cancer therapy. TNFα grafted onto AuNPs surface has reduced systemic toxicity compared to the native unconjugated TNFα. More importantly, the TNFα-AuNPs conjugates are able to accumulate preferentially in the tumor vasculature. The selective uptake of the AuNPs into the tumor has been suggested to be due to the leaky vasculature of the tumor blood vessels, which allows AuNPs of sizes ranging between 20 to 100 nm to passively diffuse into the tumor interstitium (Paciotti et al 2004). A current example of chemotherapy agents based on this technology is CYT-6091 or Aurimune™ (Figure 7) developed by CytImmune (Rockville, MD, USA) and is about to enter into phase II clinical trials for the treatment of melanoma, colorectal cancer, and urinary tract cancer. Aurimune™ is a multivalent drug consisting of 33-nm colloidal AuNPs, onto

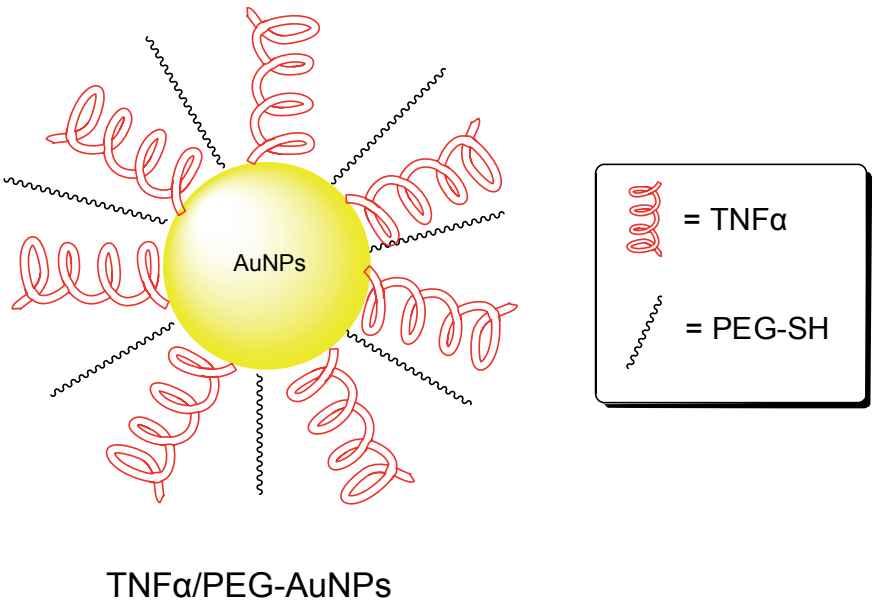

Figure 7 Illustration of TNFα/PEG-conjugated AuNPs (Aurimune-T™).

which is grafted TNFα for specific solid-tumor targeting and thiol-derivatized poly-ethylene glycol to bypass RES. Upon tumor selective uptake, the drug is internalized into tumor cells through TNFα-mediated RME (Paciotti et al 2006; Visaria et al 2006). To confirm that TNFα-binding contributes to the selectivity observed toward MC-38 tumor cells, TNFα-resistant B16/F10 melanoma cells were exposed to Aurimune™. Only temporary growth inhibition of these TNFα-resistant melanoma cells was observed (Visaria et al 2006). In addition to directing AuNPs to TNFα-specific tumor cells, TNFα also acts as an anticancer agent that induces hemorrhagic necrosis in solid tumors (North and Havell 1988; Kircheis et al 2002; Paciotti et al 2006; Visaria et al 2006).

The effect of combination of Aurimune™ with hyperthermia on cancer cell viability has also been investigated. SCK murine mammary carcinoma cells were treated with Aurimune™ and heated to 42.5 °C. In both *in vivo* and *in vitro* tumor cell survival studies, Aurimune™ at 250 μg/kg together with hyperthermia was shown to possess 2- to 3-fold higher anticancer activity compared to Aurimune™ alone (Visaria et al 2006). Possibly, the Aurimune™ hyperthermia effect induces the macro- and microvasculature shutdown (Srinivasan et al 1990; Umeno et al 1994) of the tumor cells, and consequently cuts off the blood flow that transports nutrients and oxygen to the tumors. Additionally, increase in anaerobic glycolysis in transformed cells that leads to high acidity and acidic byproducts buildup (Raghunuand et al 2003), could enhance the susceptibility of tumor cells to heat shock that resulted from hyperthermia and expedite the tumor apoptosis.

Epidermal growth factor receptor is another receptor that is overexpressed in several types of cancer including lung and pancreatic cancers (Arteaga 2001; Xiong and Abbruzzese 2002; Paez et al 2004; Ahmed and Salgia 2006; Prudkin and Wistuba 2006; Cohenuram and Saif 2007). Overexpression of EGFR has been demonstrated to culminate from mutations on EGFR gene that often proceed to uncontrolled cell division and the proliferation of cancer cells (Lynch et al 2004). Two therapeutic approaches that target EGFR-enriched cancer cells are monoclonal antibody-based therapy and tyrosine kinase inhibitors (Ahmed and Salgia 2006; Prudkin and Wistuba 2006; Cohenuram and Saif 2007). Monoclonal antibodies such as anti-EGFR antibody have been investigated as a possible anticancer therapy for lung cancer. Moreover, anti-EGFR antibody has been grafted onto 35 nm AuNPs and employed as a cancer diagnostic tool (El-Sayed et al 2005b) and for photothermal therapy (Huang et al 2007c) in an oral cancer model. Anti-EGFR–AuNPs conjugates designed for HSC and HOC oral cancer diagnostics utilized the color-scattering property of the AuNPs. When illuminated with a white light at specific angles, AuNPs, depending on their size and shape, will scatter light of many colors (Yguerabide and Yguerabide 1998). In a study aimed at diagnosis, El-Sayed and colleagues (2005b) found that anti-EGFR-AuNPs conjugates bound readily in a homogenous manner to both HOC and HSC oral cancer cell lines overexpressing EFGR. The binding of the anti-EGFR-AuNPs conjugates enabled a clear visualization of these cells under a microscope. However, HaCaT, a noncancerous cell line in which EFGR expression is depressed, only showed a random AuNPs conjugate binding. The random distribution of the conjugate leads to poor visualization, and individual HaCaT cells were undistinguishable. Such binding preferences, together with the unique light scattering property, provide a useful diagnostic tool to distinguish between noncancerous and cancerous cells. This concept has been successfully employed by Qian and colleagues (2008) to image EGFR-enriched Tu696 human head-and-neck carcinoma cells *in vivo* and *in vitro* using an ScFv version of the anti-EGFR antibody. Additionally, anti-EGFR–AuNPs conjugates have been used in photothermal therapy to target and selectively destroy EGFR-enriched cancers (El-Sayed et al 2005a; Huang et al 2006, 2007b).

Peptide delivery platforms

Most peptides used for AuNPs delivery target the cell nucleus (Table 2). The nucleus is an attractive target for photothermal therapy because it contains the cellular genetic machinery. These nuclear membrane-penetrating peptides facilitate the entry of AuNPs into the nuclei by first permitting entry into the cell via RME followed by nuclear localization through interaction with the nuclear pore complex (Tkachenko et al 2003). Most of the nuclear membrane-penetrating peptides are derived from virus sources. Common examples include the Simian virus nuclear localization peptides (NLS) (Kalderon et al 1984; Tkachenko et al 2003; Oyelere et al 2007), HIV 1 Tat-protein-derived peptides (de la Furente and Berry, 2005), and peptides derived from adenovirus fiber protein. Other nonnuclear targeting peptides that have been used as delivery vehicle for AuNPs include various forms of the RGD peptides (Tkachenko et al 2004; de la Furente et al 2006).

NLS peptides are peptides utilized by viruses to cross many cellular membranes especially the nuclear membrane. Tkachenko and colleagues have described a series of NLS peptides that are grafted onto 20-nm AuNPs (Hayat 1989; Tkachenko et al 2003, 2004; Liu et al 2007). The ability of

Table 2 Peptides utilized in AuNPs delivery

Peptide sources	Peptide sequence	Localization of peptidyl-AuNPs in cell lines	
		Cytoplasm	Nucleus
SV40 Large T NLS	CGGGPKKKRKVGG	Hela, 3T3/NIH, HepG2	HSC, HaCaT[a]
Adenoviral NLS	CGGFSTSLRARKA	3T3/NIH	Hela
Adenoviral RME	CKKKKKKSEDEYPYVPN	HepG2	N/A[c]
Adenoviral fiber protein	CKKKKKKSEDEYPYVPNFSTSLRARKA	N/A[c]	HepG2
HIV I Tat protein NLS	GRKKRRQRRR	Hela, HepG2	HFC[b]
Integrin binding domanin (RGD) + oligolysine residues	CKKKKKKGGRGDMFG	3T3/NIH	HeLa, HepG2
Synthetic RGD peptides	GRGDSP	HFC[b]	N/A[c]

Abbreviations: [a]HaCaT, noncancerous human HaCaT cells; [b]HFC, human fibroblast cells; [c]N/A, not available.

these NLS-AuNPs conjugates to selectively accumulate into the nucleus was investigated in intact Hela, 3T3/NIH, and HepG2 cells (Tkachenko et al 2004). NLS peptides derived from the SV40 large T antigen successfully facilitates the entrance of the conjugate into the nucleus of HepG2 when directly injected inside the cytoplasm (Feldherr and Akin 1990; Tkachenko et al 2003). However, the conjugates were trapped inside the cytoplasm when included in the cell growth media. This may be the result of endosome capturing of the conjugates after entrance into the cell via RME. Hence, nuclear targeting was not observed for all three cell lines (Tkachenko et al 2003, 2004). However, we recently discovered that when directly grafted onto AuNPs via a thioalkyl linker (Figure 8), NLS derived from the SV40 Large T antigen efficiently facilitated nuclear delivery of AuNPs to HSC oral cancer cells and noncancerous human HaCaT cells (Figure 9) (Oyelere et al 2007). Such discrepancy in nuclear translocation could be due to the difference in cell types or AuNPs fabrication technique.

Peptides derived from adenovirus have also been used to promote nuclear penetration (Tkachenko et al 2003, 2004). The full, single fiber protein sequence from adenovirus contains both RME and NLS domains (Tkachenko et al 2003). Its AuNPs conjugate has been shown to successfully avoid the endosome and penetrates the nucleus of the HepG2 cells (Tkachenko et al 2003, 2004). Moreover, individual RME and NLS domains derived from the adenovirus fiber protein have been independently investigated for nuclear penetration. Not surprisingly, adenoviral RME only permitted cytoplasmic delivery of AuNPs. Though adenoviral NLS sequence was incapable of entering the HepG2 cells when included in the cell media (Tkachenko et al 2003), it however facilitated transport into the cytoplasm of 3T3/NIH cells and demonstrated some evidence for nuclear translocation in Hela cells (Tkachenko et al 2004). It was concluded that the discrepancy observed with the adenoviral NLS peptides may be related to different levels of difficulty in membrane translocation among these three cell lines (Tkachenko et al 2003). Nevertheless, AuNPs grafted with a mixture of adenoviral RME and NLS sequence were shown to penetrate the nucleus of HepG2 cells (Tkachenko et al 2003). These conjugates even displayed preferential nuclear entry in comparison to the single, long adenoviral peptide that contains both RME and NLS sequence (Tkachenko et al 2003; Ryan et al 2007). The observed preference was suggested to be due to the spatial accessibility with two shorts sequences providing higher accessibility to the cellular receptors (Tkachenko et al 2003).

Similarly, the HIV 1 Tat-protein-derived peptides (Lewin et al 2000; Ford et al 2001) have facilitated the translocation of AuNPs into the nuclei of human fibroblast cells (de la Furente and Berry 2005). Tat peptide grafted onto the surface of 30 nm AuNPs via tiopronin linker successfully transported AuNPs into the nucleus with no detectable toxicity at concentration up to 10 μM. The cellular transporting pathway of Tat–tiopronin/AuNPs is similar to what was postulated for the NLS–AuNPs conjugates. Tat–AuNPs entered the cytoplasm of human fibroblast cells via RME and translocated into the nucleus through interaction with the nuclear pore.

Unlike the NLS and Tat peptides, most RGD peptides do not induce nuclear translocation. They initiate RME when bound to the RGD receptors overexpressed on the surface of human fibroblast cells. It is however important that the RGD peptide be linked through an appropriate linking moiety as improper conjugation of RGD to the AuNPs has been observed to result in loss of RGD-mediated

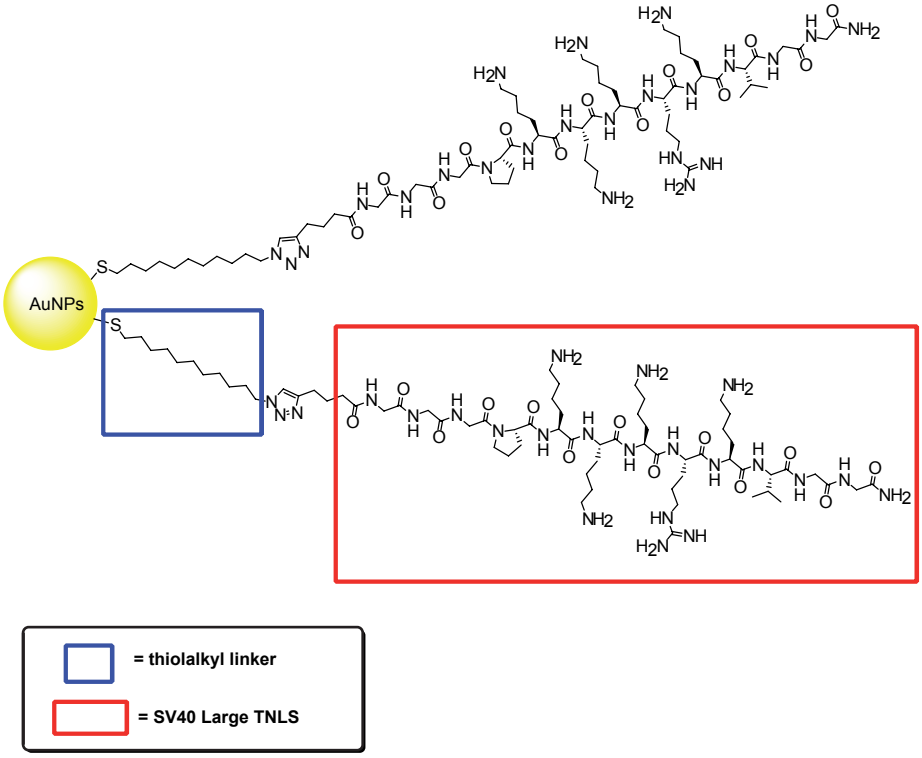

Figure 8 Illustration of SV40 Large T NLS conjugated to AuNPs surface via thiolalkyl linker.

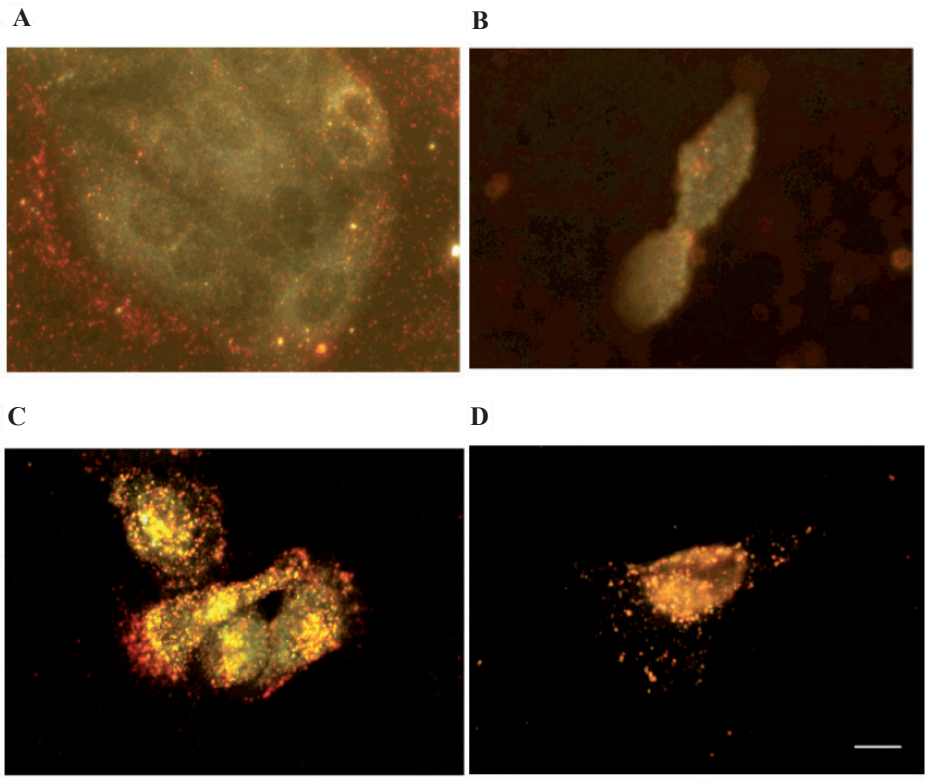

Figure 9 Dark field light scattering images of CTAB-capped Au-nanorods and SV40 largeT NLS/Au-nanorod conjugates after 2 h incubation with cells. **A**) CTAB-capped Au-nanorods in HaCaT normal cells. **B**) CTAB-capped Au-nanorods in HSC cancer cells. **C**) SV40 large T NLS/Au-nanorod conjugates in HaCaT normal cells. **D**) SV40 large T NLS/Au-nanorod conjugates in HSC cancer cells. Scale bar: 10 μm.

RME (Figure 10). For example, a direct coupling of RGD peptides via tiopronin using the same AuNPs platforms described above for the Tat–AuNPs conjugate rendered the RGD–AuNPs conjugates inactive toward human fibroblast cells. This problem could be circumvented by linking RGD peptide onto the tiopronin–AuNPs through secondary linkers, such as ethylenediamine (EDA) and poly(ethylene glycol) bis(3-aminopropyl) terminated (PEG) (Mrksich and Whitesides 1996). As expected for a RME-sequenced peptide, RGD–EDA–tiopronin–AuNPs conjugates were internalized within the cytoplasm of the human fibroblast cells. However, no internalization was observed for RGD–PEG–tiopronin–AuNPs conjugates. They remained isolated and adhered to the surface integrin receptors of the human fibroblast cells (de la Furente et al 2006). The discrepancy in RME behavior of these conjugates remained unclear and needs to be investigated further.

Despite the commonly observed lack of nuclear targeting by RGD-derived peptides, nuclear accumulation has been observed in some cell lines, including Hela and HepG2 cell, when incubated with AuNPs grafted with certain uniquely modified RGD peptides (Tkachenko et al 2004). The modified RGD peptides consist of sequence from the integrin binding domain in addition to six continuous lysine residues. The nuclear uptake of these modified RGD peptides maybe due to the resemblance of the continuous lysine residues to the lysine-enriched SV40 NLS peptides (Tkachenko et al 2004). The low toxicity of these conjugates add to the potential for their use in drug delivery, membrane receptor mapping (de la Furente et al 2006) or even photothermal therapeutic applications.

Small molecule delivery platform

AuNPs have been delivered by and/or facilitated the delivery of assorted small molecule therapeutic agents (Figure 11) into tumors. This delivery is premised on the EPR effect of AuNPs, a property that allows them to be taken up passively (via its leaky vasculature) into tumors without the assistance of targeting agents (Sahoo et al 2007). Upon accumulation at the tumor site, the appended small molecule facilitates a RME-mediated uptake of the AuNPs into the diseased cells. One example of such small molecules is folic acid, a form of water soluble vitamin B that has been exploited to selectively target folate receptor (FR) expressing tumor cells (Sudimack and Lee 2000; Lu and Low 2002; Lu et al 2004; Roy et al 2004; Stevens et al 2004). FR are overexpressed in various types of human cancers such as the ovary, kidney, breast, brain, lung, prostate, and throat, while generally absent in most normal tissues (Sudimack and Lee 2000; Lu and Low 2002; Bhattacharya et al 2007). AuNPs-folate conjugates have been shown to permit selective targeting of FR-positive tumors. These conjugates have been used in tumor imaging and photothermal therapy applications (Dixit et al 2006). Mechanistic studies of internalization of AuNPs–PEG–folate conjugates by KB cells, a human epithelial

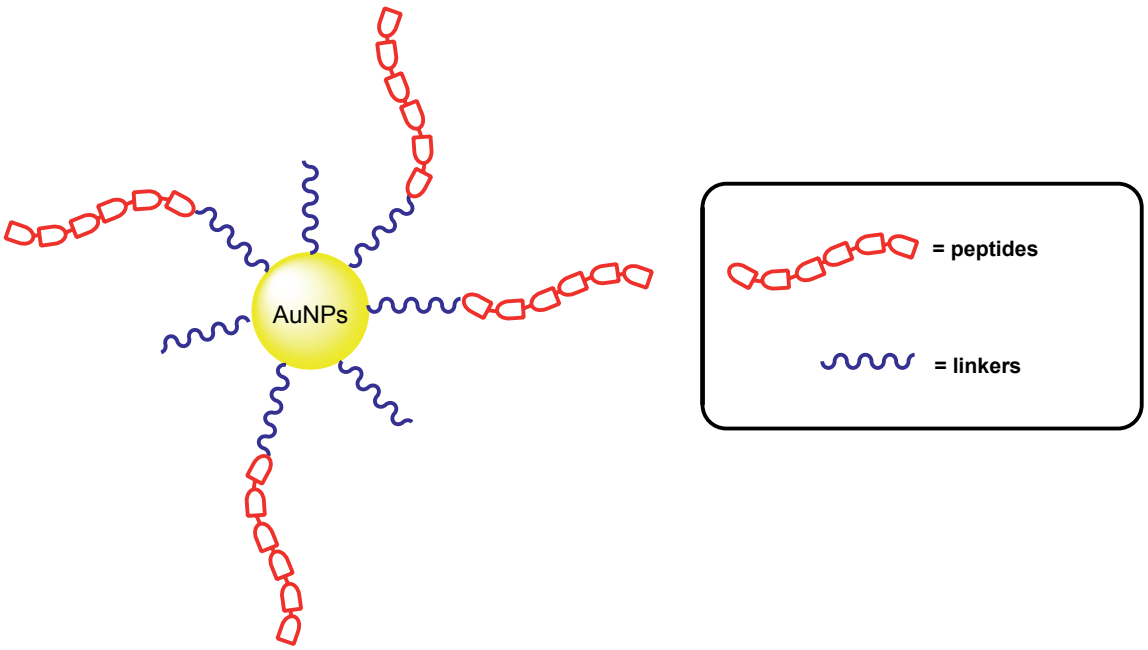

Figure 10 Illustration of peptidyl-linker conjugated AuNPs.

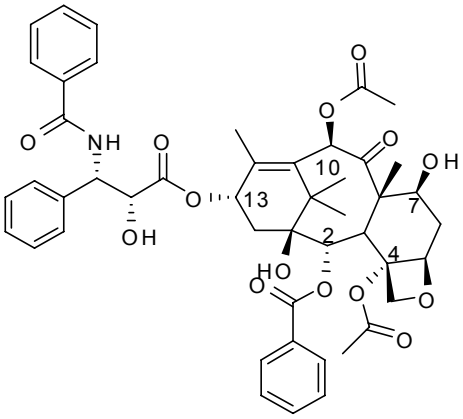

Paclitaxcel (PTX)

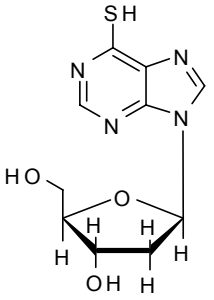

6-Mercaptopurine-9-beta-D-ribofuranoside

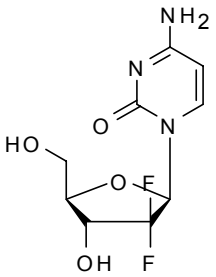

Gemcitabine

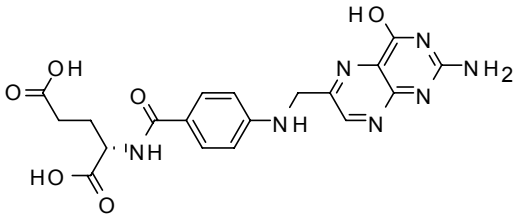

Folic acid (FA)

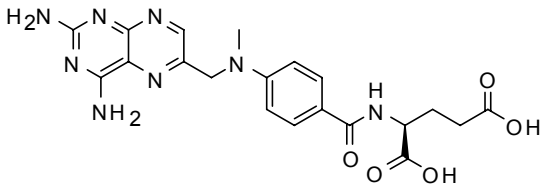

Methotrexate (MTX)

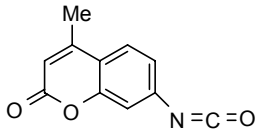

Coumarin isocyanate

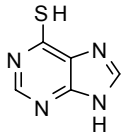

Mercaptopurine (6-MP)

Figure 1 Chemical structures of small molecules functionalized onto the surface of AuNPs.

carcinoma cell line that overexpresses the FR, revealed that the selective uptake of the conjugates is via FR-mediated RME. Dendrimer-entrapped, folate functionalized AuNPs have also shown the potential for targeting and imaging cancer cells (Shi et al 2007). Using KB cells that express both high and low levels of FR, these nanoparticles were selectively up taken by the high FR-expressing cells. Subsequent TEM imaging of treated cells revealed a predominant lysosomal localization of the nanoparticles within 2 h of incubation. A similar conjugation of AuNPs with methotrexate (MTX), an analogue of folic acid, has been reported as an alternative formulation strategy to circumvent tumor cell resistance which invariably developed upon repeated use of this versatile anticancer drug (Chen et al 2007b). It was shown that MTX–AuNPs conjugates rapidly accumulate in LL2 (Lewis lung carcinoma) cells, inducing higher cytotoxic effects on the tumor compared with free MTX which showed no antitumor effects.

AuNPs conjugates of other chemotherapeutic agents have been reported to address various limitations of the unconjugated agents (Ganesh 2007; Vijayaraghavalu et al 2007). Paciotti and colleagues recently reported a multifunctional vector for targeted drug delivery to solid tumors (Paciotti et al 2006). This vector consists of TNFα, thiolated poly(ethylene glycol) (PT), and paclitaxel (PTX),

a leading anticancer drug, which were all bound on the same 26-nm AuNPs. The release of PTX from the vector was investigated *in vitro* in B16/F10 melanoma tumor cells. It was observed that the vector remained inactive unless treated with dithiothreitol (DDT), suggesting that the vector is acting as a prodrug from which PTX must be released to elicit the desired anticancer effects. *In vivo* co-administration of cysteamine, an approved therapeutic, with the vector was found to activate PTX release. Compared to unconjugated TNFα and PTX, it was shown that the PTX–PT–AuNPs–TNFα vector delivers 10-fold more TNFα and PTX to the tumor site. A similar system, consisting of two components with different functions: an antiangiogenic molecule, VEGF antibody-2C3 (AbVF), and an anticancer drug, gemcitabine, which are both attached onto a single AuNP core, has been reported (Mukherjee et al 2005). Analysis of this conjugate using human umbilical vein endothelial cells (HUVEC) and 786-O cells revealed that the functional integrities of both VEGF antibody and gemcitabine were retained.

AuNPs have also been conjugated with clinically useful antileukemic and antiinflammatory drugs 6-mercaptopurine (6-MP) and its riboside derivative. The resulting conjugates were reported to possess substantially enhanced antiproliferative effects against K-562 leukemia cells compared to the corresponding free forms of these drugs (Podsiadlo et al 2008). In addition, AuNPs–6–MP conjugates have shown antibacterial and antifugal activities against various strains of Gram-positive and Gram-negative organisms including *Micrococcus leteus*, *Staphylococcus aureus*, *Pseudomonas aeruginosa*, *Escherichia coli*, *Aspergillus fumigatus*, and *Aspergillus niger* (Selvaraj et al 2006). This enhanced activity of 6-MP-AuNP conjugate may be attributed to the high penetrating power of AuNPs through the microorganism cell wall, their small size and high surface area. AuNPs conjugates of fluorescent small molecules, such as coumarin, have also been developed as cellular probes and delivery agents (Shenoy et al 2006). It was shown that attachment of coumarin, through a carbamate bond, to PEG-functionalized AuNPs caused significant enhancement of emission intensity. Upon incubation with MDA-MB-231 cells, the modified nanoparticles were rapidly internalized in the cells and localized in the perinuclear region as evidenced through intracellular particle tracking.

Most of the AuNPs conjugates reported in the literature have high inorganic (Au metal) contents, necessitating high nanoparticle dosages to elicit the desired effect. The availability of fabrication methods that increase the organic contents of AuNPs will not only lower their dosage-activity ratio, but also extend their utility to other applications where high loading capacity is crucial. Toward this end, Gibson and colleagues (2007) recently described a novel approach that permitted high-load functionalization of 2 nm AuNPs with PTX. The resulting hybrid nanoparticles contained a 67 wt % organic content, the highest value reported to date. If proven to be generally applicable, this method may offer an attractive alternative for the preparation of nanosized drug-delivery systems with high drug-loading capacities.

Concluding remarks

In this review, we have focused on the current applications of AuNPs in nanomedicine. We have provided an eclectic collection of AuNPs delivery strategies that are currently under investigation. Assorted classes of vehicles, including small molecules, peptides, and proteins are showing great promise in specific targeting of AuNPs to diseased tissues. In addition, the biocompatibility and photo-optical distinctiveness of AuNPs are now proven to be powerful in diagnostic and biosensing applications, thereby offering a bright hope for the diagnosis and treatment of many disease states.

The sustained fascination of the scientific community with AuNPs research have been facilitated by significant strides in many fronts including availability of a plethora of methods for the production and functionalization of AuNPs of various shapes and sizes. It is now possible to control particle sizes at nanometer resolution. Improved understanding of molecular targeting in biology has furnished several ligands that have been successfully used for specific delivery of AuNPs. With information accruing from proteomics studies on various diseases, one expects that many more ligands will be made available for AuNPs-targeted delivery.

However, the successful implementations of the promised applications of AuNPs are still limited in part by the formidable barriers imposed by the complexity of a whole organism in contrast to simple cell based studies that formed the bed rock of most of the proof-of-principle investigations. The recent results from the phase I clinical trial on Aurimune™, indicating a safe and targeted delivery of Aurimune™ in and around tumor sites (CytImmune 2008), are particularly intriguing and encouraging. This has provided very important evidence that AuNPs-based therapeutic agents could overcome the barriers presented by the human immune and circulatory systems to achieve delivery at diseased sites without uptake by healthy tissues. In principle, such improved targeted delivery could make other AuNPs-based experimental therapeutic techniques, such as photothermal therapy, practicable. With the "right" combination of delivery agents and particle size, AuNPs-based

therapeutics could effectively kill the diseased cells while eliminating the horrendous side effects of the conventional chemotherapeutic agents. Nevertheless, more still needs to be done regarding our understanding of the pharmacokinetics and toxicity profiles of AuNPs. Special attention should be given to gaining comprehensive insights on the effects of nanoparticle size, ligand conjugation and conjugation chemistry on AuNPs physiological properties. Additionally, the potential for cumulative toxicity upon repeated exposure to AuNPs-based agents must be rigorously investigated. Nanotoxicity may not be a small matter after all! Results from these and related studies will prove informative in further refinement of the design of AuNPs for use in various nanotechnology applications.

Acknowledgments

This work was financially supported by Georgia Institute of Technology and by the Blanchard fellowship to AK Oyelere. P Chen is a recipient of the GAANN predoctoral fellowship from the Georgia Tech Center for Drug Design, Development and Delivery.

References

Agarwal A, Huang SW, O'Donnell M, et al. 2007. Targeted gold nanorod contrast agent for prostate cancer detection by photoacoustic imaging. *J Appl Phys*, 102:064701–1.

Ahmed SM, Salgia R. 2006. Epidermal growth factor receptor mutations and susceptibility to targeted therapy in lung cancer. *Respirology*, 11:687–92.

Aime S, Botta M, Fasano M, et al. 1998. Lanthanide(III) chelates for NMR biomedical applications. *Chem Soc Rev*, 27:19.

Akerman ME, Chan WCW, Laakkonen P, et al. 2002. Nanocrystal targeting *in vivo*. *Proc Natl Acad Sci U S A*, 99:12617–21.

Allen TM, Hansen C, Martin F, et al. 1991. Liposomes containing synthetic lipid derivatives of poly(ethylene glycol) show prolonged circulation half-lives *in vivo*. *Biochim Biophys Acta*, 1066:29–36.

Arteaga CL. 2001. The epidermal growth factor receptor: from mutant oncogene in nonhuman cancers to terapeutic target in human neoplasia. *J Clin Oncol*, 19:32s–40s.

Aubin ME, Morales DG, Hamad-Schifferli K. 2005. Labeling ribonuclease S with a 3 nm Au nanoparticle by two-step assembly *Nano Lett*, 5:519–22.

Bakó J, Szepesi M, Márton I, et al. 2007. Synthesis of nanoparticles for dental drug delivery systems. *Fogorvosi Szemle*, 100:109–13.

Ballou B, Lagerholm BC, Ernst LA, et al. 2004. Noninvasive imaging of quantum dots in mice *Bioconjug Chem*, 15:79–86.

Baron R, Willner B, Willner I. 2007. Biomolecule–nanoparticle hybrids as functional units for nanobiotechnology. *Chem Commun*, 28:323–32.

Bernardi RJ, Lowery AR, Thompson PA, et al. 2008. Immunonanoshells for targeted photothermal ablation in medulloblastoma and glioma: an *in vitro* evaluation using human cell lines. *J Neurooncol*, 86:165–72.

Bhattacharya R, Patra CR, Earl A, et al. 2007. Attaching folic acid on gold nanoparticles using noncovalent interaction via different polyethylene glycol backbones and targeting of cancer cells. *Nanomedicine*, 3:224–38.

Boyer D, Tamarat P, Maali A, et al. 2002. Photothermal imaging of nanometer-sized metal particles among scatterers. *Science*, 297:1160–3.

Brito L, Amiji M. 2007. Nanoparticulate carriers for the treatment of coronary restenosis. *Int J Nanomedicine*, 2:143–61.

Brouckaert PG, Leroux-Roels GG, Guisez Y, et al. 1986. In vivo anti-tumour activity of recombinant human and murine TNF, alone and in combination with murine IFN-, on a syngeneic murine melanoma. *Int J Cancer*, 38:763–9.

Brown KR, Natan MJ. 1998. Hydroxylamine seeding of colloidal Au nanoparticles in solution and on surfaces. *Langmuir*, 14:726–8.

Bruchez M Jr, Moronne M, Gin P, et al. 1998. Semiconductor nanocrystals as fluorescent biological labels. *Science*, 281:2013–6.

Busbee BD, Obare SO, Murphy CJ. 2003. An improved synthesis of high-aspect-ratio gold nanorods. *J Adv Mater*, 15:414–6.

Cao YC, Jin R, Mirkin CA. 2002. Nanoparticles with raman spectroscopic fingerprints for DNA and RNA detection. *Science*, 297:1536–40.

Caravan P, Ellison JJ, McMurry TJ, et al. 1999. Gadolinium(III) chelates as MRI contrast agents: Structure, dynamics, and applications. *Chem Rev*, 99:2293–352.

Caravan P, Greenwood JM, Welch JT, et al. 2003. Gadolinium-binding helix–turn–helix peptides: DNA-dependent MRI contrast agents. *Chem Commun*, 20:2574–5.

Caruso RA, Antonietti M. 2001. Sol-gel nanocoating: An approach to the preparation of structured materials. *Chem Mater*, 13:3272–82.

Chah S, Hammond MR, Zare RN. 2005. Gold nanoparticles as a colorimetric sensor for protein conformational changes. *Chem Biol*, 12:323–8.

Chan WC, Maxwell DJ, Gao X, et al. 2002. Luminescent quantum dots for multiplexed biological detection and imaging. *Curr Opin Biotechnol*, 13:40–6.

Chen J, Saeki F, Wiley BJ, et al. 2005. Gold nanocages: bioconjugation and their potential use as optical imaging contrast agents. *Nano Lett*, 5:473–7.

Chen J, Wang D, Xi J, et al. 2007a. Immuno gold nanocages with tailored optical properties for targeted photothermal destruction of cancer cells *Nano Lett*, 7:1318–22.

Chen Y, Tsai C, Huang P, et al. 2007b. Methotrexate conjugated to gold nanoparticles inhibits tumor growth in a syngeneic lung tumor model. *Mol Pharm*, 4:713–22.

Cheng MM, Cuda G, Bunimovich YL, et al. 2006. Nanotechnologies for biomolecular detection and medical diagnostics. *Curr Opin Chem Biol*, 10:11–9.

Cho K, Wang X, Nie S, et al. 2008. Therapeutic nanoparticles for drug delivery in cancer. *Clin Cancer Res*, 14:1310–6.

Cognet L, Tardin C, Boyer D, et al. 2003. Single metallic nanoparticle imaging for protein detection in cells. *Proc Natl Acad Sci U S A*, 100:11350–5.

Cohenuram M, Saif MW. 2007. Epidermal growth factor receptor inhibition strategies in pancreatic cancer: past, present and the future. *J Pancreas*, 8:4–15.

Connor EE, Mwamuka J, Gole A, et al. 2005. Gold nanoparticles are taken up by human cells but do not cause acute cytotoxicity. *Small*, 1:325–7.

CytImmune. 2008. Aurimune™ (CYT-6091) [online]. Accessed on Sept 1, 2008. URL: http://www.cytimmune.com/go.cfm?do=Page.View&pid=26.

de la Furente JM, Berry CC, Riehle MO, et al. 2006. Nanoparticle targeting at cells. *Langmuir*, 22:3286–93.

de la Furente JM, Berry CC. 2005. Tat peptide as an efficient molecule to translocate gold nanoparticles into the cell nucleus. *Bioconjug Chem*, 16:1176–80.

De M, You C-C, Srivastava S, et al. 2007. Biomimetic interactions of proteins with functionalized nanoparticles: a thermodynamic study. *J Am Chem Soc*, 129:10747–53.

Debouttiere P-J, Roux S, Vocanson F, et al. 2006. Design of gold nanoparticles for magnetic resonance imaging. *Adv Funct Mater*, 16:2330–9.

Demann ET, Stein PS, Haubenreich JE. 2005. Gold as an implant in medicine and dentistry. *J Long Term Eff Med Implants*, 15:687–98.

Dixit V, Van den Bossche J, Sherman DM, et al. 2006. Synthesis and grafting of thioctic acid-PEG-folate conjugates onto Au nanoparticles for selective targeting of folate receptor-positive tumor cells *Bioconjug Chem*, 17:603–9.

Dong S, Roman M. 2007. Fluorescently labeled cellulose nanocrystals for bioimaging applications *J Am Chem Soc*, 129:13810–1.

Durr NJ, Larson T, Smith DK, et al. 2007. Two-photon luminescence imaging of cancer cells using molecularly targeted gold nanorods. *Nano Lett*, 7:941–5.

Edelman ER, Seifert P, Groothuis A, et al. 2001. Gold-coated NIR stents in porcine coronary arteries. *Circulation*, 103:429–34.

Elghanian R, Storhoff JJ, Mucic RC, et al. 1997. Selective colorimetric detection of polynucleotides based on the distance-dependent optical properties of gold nanoparticles. *Science*, 277:1078–81.

El-Sayed IH, Huang X, El-Sayed MA. 2005a. Selective laser photo-thermal therapy of epithelial carcinoma using anti-EGFR antibody conjugated gold nanoparticles *Cancer Lett*, 239:129–35.

El-Sayed IH, Huang X, El-Sayed MA. 2005b. Surface plasmon resonance scattering and absorption of anti-EGFR antibody conjugated gold nanoparticles in cancer diagnostics: applications in oral cancer *Nano Lett*, 5:829–34.

Everts M, Saini V, Leddon JL, et al. 2006. Covalently linked Au nanoparticles to a viral vector: potential for combined photothermal and gene cancer therapy. *Nano Lett*, 6:587–91.

Feldherr MC, Akin DJ. 1990. The permeability of the nuclear envelope in dividing and nondividing cell cultures. *J Cell Biol*, 111:1–8.

Ford KG, Souberbielle BE, Darling D, et al. 2001. Protein transduction: an alternative to genetic intervention? *Gene Ther*, 8:1–4.

Frederix F, Friedt J-M, Choi K-H, et al. 2003. Biosensing based on light absorption of nanoscaled gold and silver particles. *Anal Chem*, 75:6894–900.

Freitas RA, Jr. 2005. What is nanomedicine? *Nanomedicine*, 1:2–9.

Frens G. 1973. Controlled nucleation for the regulation of the particle size in monodisperse gold suspensions. *Nature Phys Sci*, 241:20–2.

Ganesh T. 2007. Improved biochemical strategies for targeted delivery of taxoids. *Bioorg Med Chem*, 15:3597–623.

Gao X, Cui Y, Levenson RM, et al. 2005. In vivo cancer targeting and imaging with semiconductor quantum dots. *Nat Biotechnol*, 22:969–76.

Ghoshmoulick R, Bhattacharya J, Mitra CK, et al. 2007. Protein seeding of gold nanoparticles and mechanism of glycation sensing. *Nanomedicine*, 3:208–14.

Gibson JD, Khanal BP, Zubarev ER. 2007. Paclitaxel-functionalized gold nanoparticles *J Am Chem Soc*, 129:11653–61.

Gielen M, Tiekink ERT. 2005. Metallotherapeutic Drugs and Metal-Based Diagnostic Agents: The Use of Metals in Medicine. Hoboken, NJ: John Wiley and Sons.

Goodman CM, McCusker CD, Yilmaz T, et al. 2004. Toxicity of gold nanoparticles functionalized with cationic and anionic side chains. *Bioconjug Chem*, 15:897–900.

Ha TH, Yeong JY, Chung BH. 2005. Immobilization of hexa-arginine tagged esterase onto carboxylated gold nanoparticles. *Chem Commun*, 31:3959–61.

Haba Y, Kojima C, Harada A, et al. 2007. Preparation of poly(ethylene glycol)-modified poly(amido amine) dendrimers encapsulating gold nanoparticles and their heat-generating ability. *Langmuir*, 23:5243–6.

Hainfeld JF, Slatkin DN, Focella TM, et al. 2006. Gold nanoparticles: a new X-ray contrast agent. *J Radiol*, 79:248–53.

Haller C, Hizoh I. 2004. The cytotoxicity of iodinated radiocontrast agents on renal cells in vitro. *Invest Radiol*, 39:149–54.

Han G, Ghosh P, De M, et al. 2007. Drug and gene delivery using gold nanoparticles. *NanoBioTech*, 3:40–5.

Han Y, Jiang J, Lee SS, et al. 2008. Reverse microemulsion-mediated synthesis of silica-coated gold and silver nanoparticles. *Langmuir*, 24:5842–8.

Hayat M. 1989. Colloidal Gold. Principles, Methods, and Applications. San Diego, CA: Academic Press.

Heath JR, Davis ME. 2008. Nanotechnology and cancer. *Annu Rev Med*, 59:251–65.

Herrwerth S, Eck W, Reinhardt S, et al. 2003. Factors that determine the protein resistance of oligoether self-assembled monolayers – internal hydrophilicity, terminal hydrophilicity, and lateral packing density. *J Am Chem Soc*, 125:9359–66.

Hieber U, Heim ME. 1994. Tumor necrosis factor for the treatment of malignancies. *Oncology*, 51:142–53.

Hill RT, Shear JB. 2006. Enzyme-nanoparticle functionalization of three-dimensional protein scaffolds. *Anal Chem*, 78:7022–6.

Hirsch LR, Stafford RJ, Bankson JA, et al. 2003. Nanoshell-mediated near-infrared thermal therapy of tumors under magnetic resonance guidance. *Proc Natl Acad Sci U S A*, 100:13549–54.

Hizoh I, Haller C. 2002. Radiocontrast-induced renal tubular cell apoptosis: hypertonic versus oxidative stress. *Invest Radiol*, 37:428–34.

Huaizhi Z, Yuantao N. 2001. China's ancient gold drugs. *Gold Bull*, 34:24–9.

Huang C-C, Yang Z, Chang H-T. 2004. Synthesis of dumbbell-shaped Au-Ag core-shell nanorods by seed-mediated growth under alkaline conditions. *Langmuir*, 20:6089–92.

Huang X, El-Sayed IH, Qian W, et al. 2006. Cancer cell imaging and photothermal therapy in the near-infrared region by using gold nanorods. *J Am Chem Soc*, 128:2115–20.

Huang X, Jain PK, El-Sayed IH, et al. 2007a. Gold nanoparticles: interesting optical properties and recent applications in cancer diagnostics and therapy. *Nanomed*, 2:681–93.

Huang X, Jain PK, El-Sayed IH, et al. 2008. Plasmonic photothermal therapy (PPTT) using gold nanoparticles. *Lasers Med Sci*, 23:217–28.

Huang X, Qian W, El-Sayed IH, et al. 2007b. The potential use of the enhanced nonlinear properties of gold nanospheres in photothermal cancer therapy. *Lasers Surg Med*, 39:747–53.

Hudson BI, Hofmann MA, Bucciarelli L, et al. 2002. Glycation and diabetes: The RAGE connection. *Curr Sci*, 83:1515–21.

Ipe BI, Yoosaf K, Thomas KG. 2006. Functionalized gold nanoparticles as phosphorescent nanomaterials and sensors. *J Am Chem Soc*, 128:1907–13.

Ishida O, Maruyama K, Sasaki K, et al. 1999. Size-dependent extravasation and interstitial localization of polyethyleneglycol liposomes in solid tumor-bearing mice. *Int J Pharm*, 190:49–56.

Jain KK. 2008. Nanomedicine: application of nanobiotechnology in medical practice. *Med Princ Pract*, 17:89–101.

Jain PK, Lee KS, El-Sayed IH, et al. 2006. Calculated absorption and scattering properties of gold nanoparticles of different size, shape, and composition: applications in biological imaging and biomedicine. *J Phys Chem B*, 110:7238–48.

Jana NR, Gearheart L, Murphy CJ. 2001a. Seed-mediated growth approach for shape-controlled synthesis of spheroidal and rodlike gold nanoparticles using a surfactant template. *J Adv Mater*, 13:1389–93.

Jana NR, Gearheart L, Murphy CJ. 2001b. Wet chemical synthesis of high aspect ratio cylindrical gold nanorods. *J Phys Chem B*, 105:4065–7.

Jena BK, Raj CR. 2006. Electrochemical biosensor based on integrated assembly of dehydrogenase enzymes and gold nanoparticles. *Anal Chem*, 78:6332–9.

Jin RC, Cao YW, Mirkin CA, et al. 2001. Photoinduced conversion of silver nanospheres to nanoprisms. *Science*, 294:1901–3.

Kalderon D, Richardson WD, Markham AF, et al. 1984. Sequence requirements for nuclear location of simian virus 40 large-T antigen. *Nature* (*London*), 311:33–8.

Kawasaki ES, Player A. 2005. Nanotechnology, nanomedicine, and the development of new, effective therapies for cancer. *Nanomedicine*, 1:101–9.

Khlebtsov NG, Trachuk LA, Mel'nikov AG. 2005. The effect of the size, shape, and structure of metal nanoparticles on the dependence of their optical properties on the refractive index of a disperse medium. *Opt Spectrosc*, 98:83–90.

Kim D, Park S, Lee JH, et al. 2007. Antibiofouling polymer-coated gold nanoparticles as a contrast agent for in vivo X-ray computed tomography imaging. *J Am Chem Soc*, 129:7661–5.

Kim DK, Mikhaylova M, Wang FH, et al. 2003. Starch-coated superparamagnetic nanoparticles as MR contrast agents *Chem Mater*, 15:4343–51.

Kim S, Lim YT, Soltesz EG, et al. 2004. Near-infrared fluorescent type II quantum dots for sentinel lymph node mapping. *Nat Biotechnol*, 22:93–7.

Kircheis R, Ostermann E, Wolschek MF. 2002. Tumor-targeted gene 1 of tumor necrosis factor-alpha induces tumor necrosis and tumor regression without systemic toxicity. *Cancer Gene Ther*, 9:673–80.

Kohler N, Fryxell GE, Zhang M. 2004. A bifunctional poly(ethylene glycol) silane immobilized on metallic oxide-based nanoparticles for conjugation with cell targeting agents. *J Am Chem Soc*, 126:7206–11.

Koo OM, Rubinstein I, Onyuksel H. 2005. Role of nanotechnology in targeted drug delivery and imaging: a concise review. *Nanomedicine*, 1:193–212.

Kreibig U, Genzel L. 1985. Optical absorption of small metallic particles. *Surf Sci*, 156:678–700.

Kumar CSSR. 2007. Nanomaterials for Cancer Diagnosis. Weinheim, Germany: Wiley-VCH.

Kundu S, Panigrahi S, Praharaj S, et al. 2007. Anisotropic growth of gold clusters to gold nanocubes under UV irradiation. *Nanotechnology*, 18:075712.

Kundu S, Peng L, Liang H. 2008. A new route to obtain high-yield multiple-shaped gold nanoparticles in aqueous solution using microwave radiation. *Inorg Chem*, 47:6344–52.

Langereis S, Kooistra HA, van Genderen MH, et al. 2004. Probing the interaction of the biotin – avidin complex with the relaxivity of biotinylated Gd-DTPA. *Org Biomol Chem*, 2:1271–3.

Lanza G, Winter P, Cyrus T, et al. 2006. Nanomedicine opportunities in cardiology. *Ann N Y Acad Sci*, 1080:451–65.

Lee H, Lee E, Kim DK, et al. 2006a. Antibiofouling polymer-coated superparamagnetic iron oxide nanoparticles as potential magnetic resonance contrast agents for in vivo cancer imaging. *J Am Chem Soc*, 128:7383–9.

Lee JH, Huh M, Jun YW, et al. 2006b. Artificially engineered magnetic nanoparticles for ultra-sensitive molecular imaging. *Nat Med*, 13:95–9.

Lee K-S, El-Sayed MA. 2006. Gold and silver nanoparticles in sensing and imaging: sensitivity of plasmon response to size, shape, and metal composition. *J Phys Chem B*, 110:19220–5.

Lee LA, Wang Q. 2006. Adaptations of nanoscale viruses and other protein cages for medical applications. *Nanomedicine*, 2:137–49.

Lewin M, Carlesso N, Tung C-H, et al. 2000. Tat peptide-derivatized magnetic nanoparticles allow in vivo tracking and recovery of progenitor cells. *Nat Biotechnol*, 18:410–4.

Lewinski N, Colvin V, Drezek R. 2008. Cytotoxicity of nanoparticles. *Small*, 4:26–49.

Lewis DJ, Day TM, MacPherson JV, et al. 2006. Luminescent nanobeads: attachment of surface reactive Eu(III) complexes to gold nanoparticles. *Chem Commun*, 13:1433–5.

Li H, Rothberg L. 2004. Colorimetric detection of DNA sequences based on electrostatic interactions with unmodified gold nanoparticles. *Proc Natl Acad Sci U S A*, 101:14036–9.

Liu Y, Shipton MK, Kaufman ED, et al. 2007. Synthesis, stability, and cellular internalization of gold nanoparticles containing mixed peptide-poly(ethylene glycol) monolayers. *Anal Chem*, 79:2221–9.

Loo C, Lowery A, Halas N, et al. 2005. Immunotargeted nanoshells for integrated cancer imaging and therapy. *Nano Lett*, 5:709–11.

Lowery AR, Gobin AM, Day ES, et al. 2006. Immunonanoshells for targeted photothermal ablation of tumor cells. *Int J Nanomedicine*, 1:149–54.

Lu C-W, Hung Y, Hsiao J-K, et al. 2007. Bifunctional magnetic silica nanoparticles for highly efficient human stem cell labeling. *Nano Lett*, 7:149–54.

Lu L, Wang H, Zhou Y, et al. 2002. Seed-mediated growth of large, monodisperse core – shell gold – silver nanoparticles with Ag-like optical properties. *Chem Commun*, 2:144–5.

Lu Y, Low PS. 2002. Folate-mediated delivery of macromolecular anticancer therapeutic agents. *Adv Drug Deliv Rev*, 54:675–93.

Lu Y, Sega E, Leamon CP, et al. 2004. Folate receptor-targeted immunotherapy of cancer: mechanism and therapeutic potential. *Adv Drug Deliv Rev*, 56:1161–76.

Lynch TJ, Bell DW, Sordella R, et al. 2004. Activating mutations in the epidermal growth factor receptor underlying responsiveness of non-small-cell lung cancer to gefitinib. *N Engl J Med*, 350:2129–39.

Maeda H, Wu J, Sawa T, et al. 2000. Tumor vascular permeability and the EPR effect in macromolecular therapeutics: a review. *J Control Release*, 65:271–84.

Mahmood U, Weissleder R. 2003. Near-infrared optical imaging of proteases in cancer. *Mol Cancer Ther*, 2:489–96.

Majoros IJ, Myc A, Thomas T, et al. 2006. PAMAM dendrimer-based multifunctional conjugate for cancer therapy: synthesis, characterization, and functionality. *Biomacromolecules*, 7:572–9.

Marinakos SM, Novak JP, Brousseau LC, et al. 1999. Gold particles as templates for the synthesis of hollow polymer capsules. control of capsule dimensions and guest encapsulation. *J Am Chem Soc*, 121:8518–22.

Martina MS, Fortin JP, Menager C, et al. 2005. Generation of superparamagnetic liposomes revealed as highly efficient MRI contrast agents for in vivo imaging. *J Am Chem Soc*, 127:10676–85.

Maysinger D. 2007. Nanoparticles and cells: good companions and doomed relationships. *Org Biomol Chem*, 5:2335–42.

McFadden P. 2002. Broadband biodetection: Holmes on a chip. *Science*, 297:2075–6.

Merbach A, Toth E. 2001. The Chemistry of Contrast Agent in Magnetic Resonance Imaging. Chichester, UK: Wiley.

Mitra RN, Das PK. 2008. In situ preparation of gold nanoparticles of varying shape in molecular hydrogel of peptide amphiphiles. *J Phys Chem C*, 112:8159–66.

Moolhuizen G, Paciotti GF, de Leede LGJ, et al. 2004. Colloidal gold nanoparticles. London, UK: Business Briefing, Pharmatech.

Morrow KJJ, Bawa R, Wei C. 2007. Recent advances in basic and clinical nanomedicine. *Med Clin North Am*, 91:805–43.

Mrksich M, Whitesides GM. 1996. Using self-assembled monolayers to understand the interactions of man-made surfaces with proteins and cells. *Annu Rev Biophys Biomol Struct*, 25:55–78.

Mu L, Feng SS. 2003. A novel controlled release formulation for the anticancer drug paclitaxel (Taxol®): PLGA nanoparticles containing vitamin E TPGS. *J Control Release*, 86:33–48.

Mukherjee P, Bhattacharya R, Mukhopadhyay D. 2005. Gold nanoparticles bearing functional anti-cancer drug and anti-angiogenic agent: A "2 in 1" system with potential application in cancer therapeutics. *J Biomed Nanotech*, 1:224–8.

Murphy CJ, Jana NR. 2002. Controlling the aspect ratio of inorganic nanorods and nanowires. *Adv Mater*, 14:80–2.

Nasongkla N, Bey E, Ren J, et al. 2006. Multifunctional polymeric micelles as cancer-targeted, MRI-ultrasensitive drug delivery systems. *Nano Lett*, 6:2427–30.

[NCI] National Cancer Institute. 2003. Computed tomography (CT): Questions and answers [online]. Accessed on Sept 1, 2008. URL: http://www.cancer.gov/cancertopics/factsheet/Detection/CT.

Nicholas JD, Larson T, Smith DK, et al. 2007. Two-photon luminescence imaging of cancer cells using molecularly targeted gold nanorods. *Nano Lett*, 7:941–5.

Niidome T, Yamagata M, Okamoto Y, et al. 2006. PEG-modified gold nanorods with a stealth character for in vivo applications *J Control Release*, 114:343–7.

North RJ, Havell EA. 1988. The antitumor function of tumor necrosis factor (TNF) II. Analysis of the role of endogenous TNF in endotoxin-induced hemorrhagic necrosis and regression of an established sarcoma. *J Exp Med*, 167:1086–99.

Okazaki K-I, Kiyama T, Hirahara K, et al. 2008. Single-step synthesis of gold – silver alloy nanoparticles in ionic liquids by a sputter deposition technique. *Chem Commun*, 6:691–3

Otsuka H, Akiyama Y, Nagasaki Y, et al. 2001. Quantitative and reversible lectin-induced association of gold nanoparticles modified with -lactosyl – mercapto-poly(ethylene glycol). *J Am Chem Soc*, 123:8226–30.

Oyelere AK, Chen PC, Huang X, et al. 2007. Pepetide-conjugated gold nanorods for nuclear targeting. *Bioconjug Chem*, 18:1490–7.

Paciotti GF, Kingston DGI, Tamarkin L. 2006. Colloidal gold nanoparticles: a novel nanoparticle platform for developing multifunctional tumor-targeted drug delivery vectors. *Drug Dev Res*, 67:47–54.

Paciotti GF, Myer L, Weireich D, et al. 2004. Colloidal gold: a novel nanoparticle vector for tumor directed drug delivery. *Drug Deliv*, 11:169–83.

Paez JP, Janne PA, Lee JC, et al. 2004. EGFR mutations in lung cancer: correlation with clinical response to gefitinib therapy. *Science*, 304:1497–500.

Pal A, Esumi K. 2007. Photochemical synthesis of biopolymer coated Aucore-Agshell type bimetallic nanoparticles. *J Nanosci Nanotechnol*, 7:2110–5.

Pal S, De G. 2007. Synthesis of Au-Ag alloy nanoparticles with Au/Ag compositional control in SiO_2 film matrix. *J Nanosci Nanotechnol*, 7:1994–9.

Pan Y, Neuss S, Leifert A, et al. 2007. Size-dependent cytotoxicity of gold nanoparticles. *Small*, 3:1941–9.

Pandey P, Singh SP, Arya SK, et al. 2007. Application of thiolated gold nanoparticles for the enhancement of glucose oxidase activity. *Langmuir*, 23:3333–7.

Papahadjopoulos D, Allen TM, Gabizon A, et al. 1991. Sterically stablized liposomes: improvements in pharmacokinetics and antitumor therapeutic efficacy. *Proc Natl Acad Sci U S A*, 88:11460–4.

Peters R. 2006. Nanoscopic medicine: The next frontier. *Small*, 2:452–6.

Pissuwan D, Valenzuela SM, Miller CM, et al. 2007. A golden bullet? Selective targeting of toxoplasma gondii tachyzoites using antibody-functionalized gold nanorods. *Nano Lett*, 7:3808–12.

Podsiadlo P, Sinani VA, Bahng JH, et al. 2008. Gold nanoparticles enhance the anti-leukemia action of a 6-mercaptopurine chemotherapeutic agent. *Langmuir*, 24:568–74.

Prato M, Kostarelos K, Bianco A. 2008. Functionalized carbon nanotubes in drug design and discovery. *Acc Chem Res*, 41:60–8.

Prudkin L, Wistuba II. 2006. Epidermal growth factor receptor abnomalities in lung cancer. Pathogentic and clinical implications. *Ann Diagn Pathol*, 10:306–15.

Pulliam B, Sung JC, Edwards DA. 2007. Design of nanoparticle-based dry powder pulmonary vaccines. *Expert Opin Drug Deliv*, 4:651–63.

Pyrpassopoulos S, Niarchos D, Nouneis G, et al. 2007. Synthesis and self-organization of Au nanoparticles. *Nanotechnology*, 18:485604.

Qian X, Peng X-H, Ansari DO, et al. 2008. *In vivo* tumor targeting and spectroscopic detection with surface-enhanced Raman nanoparticle tags. *Nat Biotechnol*, 26:83–90.

Raghunuand N, Gatenby RA, Gillies RJ. 2003. Microenvironmental and cellular consequences of altered blood flow in tumours. *Br J Radiol*, 76:S11–S22.

Ragusa A, García I, Penadés S. 2007. Nanoparticles as nonviral gene delivery vectors. *IEEE Trans Nanobioscience*, 6:319–30.

Rawat M, Singh D, Saraf S. 2006. Nanocarriers: promising vehicle for bioactive drugs. *Biol Pharm Bull*, 29:1790–8.

Raynal I, Prigent P, Peyramaure S, et al. 2004. Macrophage endocytosis of superparamagnetic iron oxide nanoparticles: mechanisms and comparison of ferumoxides and ferumoxtran-10. *Invest Radiol*, 39:56–63.

Richards DG, McMIllin DL, Mein EA, et al. 2002. Gold and its relationship to neurological/glandular conditions. *Int J Neurosci*, 112:31–53.

Roger WJ, Basu P. 2005. Factors regulating macrophage endocytosis of nanoparticles: implications for targeted magnetic resonance plaque imaging. *Atherosclerosis*, 178:67–73.

Roy EJ, Gawlick U, Orr BA, et al. 2004. Folate-mediated targeting of T cells to tumors. *Adv Drug Deliv Rev*, 56:1219–31.

Ryan JA, Overton KW, Speight ME, et al. 2007. Cellular uptake of gold nanoparticles passivated with BSA-SV40 large t antigen conjugates. *Anal Chem*, 79:9150–9.

Sahoo SK, Labhasetwar V. 2003. Nanotech approaches to drug delivery and imaging. *Drug Discov Today*, 8:1112–20.

Sahoo SK, Parveen S, Panda JJ. 2007. The present and future of nanotechnology in human health care. *Nanomedicine*, 3:20–31.

Sarkar D, Halas NJ. 1997. General vector basis function solution of Maxwell's equations. *Phys Rev E*, 56:1102.

Sato K, Hosokawa K, Maeda M. 2003. Rapid aggregation of gold nanoparticles induced by non-cross-linking DNA hybridization. *J Am Chem Soc*, 125:8102–3.

Sato K, Hosokawa K, Maeda M. 2005. Non-cross-linking gold nanoparticle aggregation as a detection method for single-base substitutions. *Nucleic Acids Res*, 33:e4.

Sau TK, Murphy CJ. 2004. Room temperature, high-yield synthesis of multiple shapes of gold nanoparticles in aqueous solution. *J Am Chem Soc*, 126:8648–9.

Selvaraj V, Alagar M, Hamerton I. 2006. Analytical detection and biological assay of antileukemic drug using gold nanoparticles. *Electrochim Acta*, 52:1152–60.

Sharma P, Brown S, Walter G, et al. 2006. Nanoparticles for bioimaging. *Adv Colloid Interface Sci*, 123–6:471–85.

Shaw III FC. 1999. Gold-based therapeutic agents. *Chem Rev*, 99:2589–600.

Shenoy D, Fu W, Li J, et al. 2006. Surface functionalization of gold nanoparticles using hetero-bifunctional poly(ethylene glycol) spacer for intracellular tracking and delivery. *Int J Nanomedicine*, 1:51–7.

Shi X., Wang S, MeshinchI S, et al. 2007. Dendrimer-entrapped gold nanoparticles as a platform for cancer-cell targeting and imaging. *Small*, 3:1245–52.

Shukla R, Bansal V, Chaudhary M, et al. 2005. Biocompatibility of gold nanoparticles and their endocytotic fate inside the cellular compartment: a microscopic overview. *Langmuir*, 21:10644–54.

Simonian AL, Good TA, Wang S-S, et al. 2005. Nanoparticle-based optical biosensors for the direct detection of organophosphate chemical warfare agents and pesticides. *Anal Chim Acta*, 534:69–77.

Skrabalak SE, Au L, Lu X, et al. 2007. Gold nanocages for cancer detection and treatment. *Nanomed*, 2:657–68.

Sonnichsen C, Franzl T, Wilk T, et al. 2002. Drastic reduction of plasmon damping in gold nanorods. *Phys Rev Lett*, 88:077402.

Srinivasan JM, Fajardo LF, Hahn GM. 1990. Mechanism of antitumor activity of tumor necrosis factor alpha with hyperthermia in a tumor necrosis factor alpha-resistant tumor. *J Natl Cancer Inst*, 82:1904–10.

Stevens PJ, Sekido M, Lee RJ. 2004. A folate receptor-targeted lipid nanoparticle formulation for a lipophilic paclitaxel prodrug. *Pharm Res*, 21:2153–7.

Stonehuerner JG, Zhao J, O'Daly JP, et al. 1992. Comparison of colloidal gold electrode fabrication methods: the preparation of a horseradish peroxidase enzyme electrode. *Biosens Bioelectron*, 7:421–8.

Streicher RM, Schmidt M, Fiorito S. 2007. Nanosurfaces and nanostructures for artificial orthopedic implants. *Nanomed*, 2:861–74.

Sudimack J, Lee RJ. 2000. Targeted drug delivery via the folate receptor. *Adv Drug Deliv Rev*, 41:147–62.

Sun RW, Ma DL, Wong EL, et al. 2007. Some uses of transition metal complexes as anti-cancer and anti-HIV agents. *Dalton Trans*, 43:4884–92.

Sun Y, Mayers B, Xia Y. 2003. Metal nanostructures with hollow interiors. *Adv Mater*, 15:641–6.

Sun Y, Xia Y. 2003. Gold and silver nanoparticles: A class of chromophores with colors tunable in the range from 400 to 750 nm. *Analyst*, 128:686–91.

Svedman C, Dunér K, Kehler M, et al. 2006. Lichenoid reactions to gold from dental restorations and exposure to gold through intracoronary implant of a gold-plated stent. *Clin Res Cardiol*, 95:689–91.

Svedman C, Tillman C, Gustavsson CG, et al. 2005. Contact allergy to gold in patients with gold-plated intracoronary stents. *Contact Dermatitis*, 52:192–6.

Thelen A, Bauknecht HC, Asbach P, et al. 2006. Behavior of metal implants used in ENT surgery in 7 Tesla magnetic resonance imaging. *Eur Arch Otorhinolaryngol*, 263:900–5.

Thurn KT, Brown EMB, Wu A, et al. 2007. Nanoparticles for applications in cellular imaging. *Nanoscale Res Lett*, 2:430–41.

Tkachenko AG, Xie H, Coleman D, et al. 2003. Multifunctional gold nanoparticle-peptide complexes for nuclear targeting. *J Am Chem Soc*, 125:4700–1.

Tkachenko AG, Xie H, Coleman D, et al. 2004. Cellular trajectories of peptide-modified gold particle complexes: comparison of nuclear localization signals and peptide transduction domains. *Bioconjug Chem*, 15:482–90.

Torchilin VP, Lukyanov AN, Gao Z, et al. 2003. Immunomicelles: Targeted pharmaceutical carriers for poorly soluble drugs. *Proc Natl Acad Sci U S A*, 100:6039–44.

Tsai CS, Yu TB, Chen CT. 2005. Gold nanoparticle-based competitive colorimetric assay for detection of protein–protein interactions. *Chem Commun*, 34:4273–5.

Turkevich J, Stevenson PC, Hillier J. 1951. A study of the nucleation and growth process in the synthesis of colloidal gold. *Discuss Faraday Soc*, 11:55–75.

Umeno H, Watanabe H, Yamauchi N, et al. 1994. Enhancement of blood stasis and vascular permeability in Meth-A tumors by administration of hyperthermia in combination with tumor necrosis factor. *Jpn J Cancer Res*, 85:325–30.

Vijayaraghavalu S, Raghavan D, Labhasetwar V. 2007. Nanoparticles for delivery of chemotherapeutic agents to tumors. *Curr Opin Investig Drugs*, 8:477–84.

Villalonga R, Cao R, Gragoso A. 2007. Supramolecular chemistry of cyclodextrin in enzyme technology. *Chem Rev*, 107:3088–116.

Visaria RK, Griffin RJ, Williams BW, et al. 2006. Enhancement of tumor thermal therapy using gold nanoparticle-assisted tumor necrosis factor-alpha delivery. *Mol Cancer Ther*, 5:1014–20.

Wang H, Huff TB, Zweifel DA, et al. 2005. *In vitro* and *in vivo* two photon luminescence imaging of single gold nanorods. *Proc Natl Acad Sci U S A*, 102:15752–6.

Weissleder R, Mahmood U. 2001. Molecular imaging. *Radiology*, 219:316–33.

Woodle MC, Engbers CM, Zalipsky S. 1994. New amphipatic polymer-lipid conjugates forming long-circulating reticuloendothelial system-evading liposomes. *Bioconjug Chem*, 5:493–6.

Xiong HQ, Abbruzzese IL. 2002. Epidermal growth factor receptor-targeted therapy for pancreatic cancer. *Semin Oncol*, 29:31–7.

Yang PH, Sun X, Chiu JF, et al. 2005. Transferrin-mediated gold nanoparticle cellular uptake. *Bioconjug Chem*, 16:494–6.

Yeh HC, Ho YP, Wang TH. 2005. Quantum dot – mediated biosensing assays for specific nucleic acid detection. *Nanomedicine*, 1:115–21.

Yguerabide J, Yguerabide EE. 1998. Light-scattering submicroscopic particles as highly fluorescent analogs and their use as tracer labels in clinical and biological applications II. experimental characterization. *Anal Biochem*, 262:157–76.

Zhao W, Jeffrey CFL, Chiuman W, et al. 2008. Enzymatic cleavage of nucleic acids on gold nanoparticles: a generic platforms for facile colorimetric biosensors. *Small*, 4:810–6.

Zharov VP, Kim JW, Curiel DT, et al. 2005. Self-assembling nanoclusters in living systems: application for integrated photothermal nanodiagnostics and nanotherapy. *Nanomedicine*, 1:326–45.

Zheng M, Davidson F, Huang X. 2003. Ethylene glycol monolayer protected nanoparticles for eliminating nonspecific binding with biological molecules. *J Am Chem Soc*, 125:7790–1.